Natural Hazards
https://doi.org/10.1007/s11069-021-04624-w

ORIGINAL PAPER

ReNovRisk: a multidisciplinary programme to study the cyclonic risks in the South-West Indian Ocean

Pierre Tulet[1] · Bertrand Aunay[2] · Guilhem Barruol[3,4] · Christelle Barthe[1] · Remi Belon[2] · Soline Bielli[1] · François Bonnardot[5] · Olivier Bousquet[1] · Jean-Pierre Cammas[1,6] · Julien Cattiaux[7] · Fabrice Chauvin[7] · Idriss Fontaine[8] · Fabrice R. Fontaine[3,9] · Franck Gabarrot[6] · Sabine Garabedian[8] · Alicia Gonzalez[3,4] · Jean-Lambert Join[3] · Florian Jouvenot[10] · David Nortes-Martinez[8] · Dominique Mékiès[1] · Pascal Mouquet[10] · Guillaume Payen[6] · Gwenaelle Pennober[10] · Joris Pianezze[1] · Claire Rault[2] · Christophe Revillion[10] · Elisa J. Rindraharisaona[3,4] · Kevin Samyn[2] · Callum Thompson[1] · Hélène Vérèmes[1,6]

Received: 13 October 2020 / Accepted: 3 February 2021

Abstract
Today, resilience in the face of cyclone risks has become a crucial issue for our societies. With climate change, the risk of strong cyclones occurring is expected to intensify significantly and to impact the way of life in many countries. To meet some of the associated challenges, the interdisciplinary ReNovRisk programme aims to study tropical cyclones and their impacts on the South-West Indian Ocean basin. This article is a presentation of the ReNovRisk programme, which is divided into four areas: study of cyclonic hazards, study of erosion and solid transport processes, study of water transfer and swell impacts on the coast, and studies of socio-economic impacts. The first transdisciplinary results of the programme are presented together with the database, which will be open access from mid-2021.

Keywords Tropical cyclone · Cyclonic hazards · Interdisciplinary programme · Indian Ocean

1 Introduction

The South-West Indian Ocean (SWIO) is the second-to-third most active tropical cyclone basin in the world. Approximately 10%–12% of the world's total cyclonic activity takes place in the SWIO, where two regions are particularly involved: the Mozambique Channel and the open ocean east of Madagascar (Neumann et al. 1993). Mavume et al. (2008) and Leroux et al. (2018) confirmed this high activity and showed that the basin has an annual average of 9 to 10 tropical storms, half of which develop into

✉ Pierre Tulet
pierre.tulet@univ-reunion.fr

Extended author information available on the last page of the article

tropical cyclones (TC). Particularly intense TCs have developed in this part of the world recently. Very Intense Tropical Cyclone (VITC, WMO (2016), maximum of the average wind speed greater than 60 m s^{-1}; Hellen (2014)) and Intense Tropical Cyclone (ITC, maximum of the average wind speed between 46 and 59 m s^{-1}); Kenneth (2020)) were the two most intense tropical cyclones ever observed in the Mozambique Channel. More recently, ITC Idai (2019) caused more than 1000 deaths in Mozambique. VITC Fantala (2016) was the second most intense tropical cyclone ever recorded in the whole basin and devastated the Farquhar archipelago of the Seychelles. VITC Gafilo (2004) made landfall first on the north-eastern region of Madagascar and then on its south-western part, affecting more than 200 000 people and killing more than 350. In 2017, ITC Enawo also landed in North-East Madagascar and killed ~ 50 people (more than 300 000 people affected).

Two essential elements make the SWIO particularly sensitive to cyclonic risks. The first is large number of developing countries with fragile infrastructures and food and water supply systems, where a significant proportion of the population is living in extreme poverty. The second is due to the topography of some regions in the basin. Several islands of volcanic origin have steep slopes that locally reinforce convection, wind channelling effects and precipitation. Reunion Island, for instance, lays claim to several world records for cumulative rainfall: 1.1 m and 1.8 m over 12 h and 24 h, respectively, for TC Denise in 1966 (Holland 1993), and 3.9 m and 4.9 m over 72 h and 96 h, respectively, for TC Gamède in 2007 (Quetelard et al. 2007). Its orography has been shown to significantly influence the track and intensity of TCs passing nearby (Barbary et al. 2019). Terry et al (2013) also showed that in January and February a large proportion of storms in the SWIO had curving and sinuously moving trajectories. This track sinuosity is found to increase the storm longevity and the difficulties in forecasting, which reinforce the exposure of the territories.

Such intense precipitation generates landslides, ground movements and flash floods. In general, following the passage of a cyclone, several hundreds of landslides can impact the infrastructures (more than 200 landslides, rock falls or erosion phenomena were counted during TC Berguitta (2018) in Reunion Island (Aunay et al. 2018)). Sudden slope collapses and accelerations of slow-moving landslides are driven by the duration and intensity of precipitation (e.g. Caine 1980; Iverson 2000). Beyond the number of landslides, the moving masses involved can be considerable: two landslides of over 350 Mm^3 each, in the Salazie area of Reunion Island, move up to 1 m per year and more than 1,000 people live directly on their surfaces (Belle et al. 2014).

In some regions of Mozambique and Madagascar, which have vast plains or highlands as well as catchment areas sensitive to flooding, the impact of cyclonic rainfall can be particularly tragic. In 2019, for instance, floods caused by the landfall of TC Idai affected more than 2.6 million people in Mozambique, Malawi and Zimbabwe, with a devastating cost in human lives (more than 1000 deaths and 2450 persons declared missing), as well as significant economic damage (2 billion dollars estimated in 2019). Furthermore, TCs induce indirect economic impacts—both in time and space, and throughout the different levels of the economic fabric—whose magnitudes may compete with direct ones (Camargo and Hsiang 2015; Meyer et al. 2013). Such phenomena are especially relevant in the context of the SWIO insofar as the combination of both kinds of economic impacts has the potential to compromise a given country's long-term capacity to grow and develop (Hsiang and Jina 2014).

Regarding the strong impact of cyclonic hazards on lives and territories of the SWIO, a crucial question arises concerning the evolution of this risk with climate change. One

key aspect is the expected increase in ocean temperatures, future projections for which are described by the Intergovernmental Panel for Climate Change (IPCC). According to their scenario RCP8.5 describing "business-as-usual" high emissions, CMIP5 and CMIP6 climate models (i.e. those in the Coupled Model Intercomparison Project Phases 5 and 6) predict a global average increase in ocean surface temperatures of 2.6 °C–4.8 °C by 2100 (ICCP, 2013). In the SWIO basin, this increase could exceed 4 °C in the northern Mozambique Channel and have the direct consequence of significantly increasing the energy available for TCs. Associated with this temperature evolution, the tropical band delineated by the seasonal displacement of the inter-tropical convergence zone is expanding by 0.25°–0.5° latitude per decade (Lu et al. 2009; Staten et al. 2018, 2020). This expansion significantly widens the geographical zones conducive to cyclogenesis and thus increases the potential for cyclonic impacts on territories that are currently at low risk. It also affects the evolution of cyclone intensity. Kosin et al. (2014) highlight a year-on-year poleward shift in the latitude at which cyclones reach their lifetime maximum intensity. More recently, based on an analysis of 39 years of data, Kosin et al. (2020) have shown an 8% increase per decade in the occurrence of the most intense cyclones (categories 3–5 on the Saffir–Simpson scale).

High-resolution numerical modelling studies that re-simulate historical cyclones using projected future climates also point to an increase in cyclone risk. Most studies highlight an increase in intensity of the order of 10 hPa and an increase in precipitation of 15%–27% (Lackmann 2015; Parker et al. 2018; Mittal et al. 2019). However, to date, no regional or mesoscale studies have been carried out to study the climatic evolution of cyclone hazard in the SWIO basin.

With regard to future cyclone risk, in its AR5 report of 2014 (Impacts, Adaptation and Vulnerability, https://www.ipcc.ch/report/ar5/wg2/), the IPCC recommends (i) strengthening early warning capabilities, (ii) developing cyclone and flood shelters, (iii) improving building codes and practices, (iv) strengthening transport systems and road infrastructure, and (v) developing rainwater and wastewater management.

In response to some of these challenges, the ReNovRisk programme (REunion NOVative research on cyclonic RISKs, € 6 M) was launched in 2017. It is funded by the European Union (FEDER and INTER-REG5 funds), Région Reunion, the French government (CPER funds), the BRGM (French Geological Survey), and the CNRS (French National Centre for Scientific Research). ReNovRisk is developing an integrated study of the various risks associated with tropical cyclones in the SWIO basin by integrating mapping and economic analysis of the damage.

Coordinated by the Université de La Reunion, BRGM and IRD (French Research Institute for Development), ReNovRisk brings together a large consortium of research laboratories and scientific institutes from several countries in the western Indian Ocean, including France, Madagascar, the Seychelles, Mozambique, and Mauritius. Drawing on this wide pool of resources and expertise, the objectives of the ReNovRisk programme are multiple: (i) to improve observations and numerical forecasting systems for tropical cyclones in the SWIO, (ii) to study the cyclonic risks associated with winds, rainfall, ground movements, floods, submersion and swell over several target regions, and (iii) to develop a methodology suited to the SWIO that can estimate the direct and indirect economic costs associated with cyclonic damage.

This article is intended to present an overview of the ReNovRisk programme by detailing the presentation and strategy of its sub-programmes (Sect. 2). Some preliminary results from the various sub-programmes are presented in Sect. 3, and the ReNovRisk open databases are described in Sect. 5.

2 Organization and strategy of ReNovRisk programmes

The ReNovRisk programme is divided into four interactive sub-programmes (Fig. 1). ReNovRisk-Cyclone (RNR-C) is divided into two components referred to as "Cyclones and Climate Change" and "Cyclones and Precipitation". It aims to (i) improve the spatial coverage of TC observations over the SWIO, (ii) develop high-resolution TC forecasting models and (ii) analyse future TC activity at both basin and local scale from high-resolution climate and mesoscale simulations. The RNR-C outputs feed the other ReNovRisk programmes with swell fields, high-resolution winds and precipitation and also climate projections on the intensity and occurrence of cyclones. The aim of ReNovRisk-Erosion (RNR-E) is to study landslides, floods and solid transport in two sensitive catchment areas of Reunion Island. ReNovRisk-Transfer (RNR-T) analyses the transfer and connection of cyclonic risks across the western volcanic plateau of Reunion Island, which slopes down through temporary semi-urbanized ravines (flood risks) to the coastline of either the ocean or the back reef lagoon (risks of sediment transport, erosion, and submersion). RNR-T also provides other ReNovRisk programmes with high-resolution maps of rainfall over Reunion Island. ReNovRisk-Impacts (RNR-I) aims at mapping and analysing the economic vulnerability of, and the damage caused by TC in Reunion Island and Madagascar. Furthermore, RNR-I also approaches societal impacts of TC. The geographic area of the ReNovRisk programmes is shown in Fig. 2.

2.1 ReNovRisk-cyclone (RNR-C)

Given the colossal impact of TCs on local populations, infrastructures and economic development in the SWIO, it is essential to improve the prediction of cyclonic events at all spatial and temporal scales in order to adapt public development policies to the present and future risks faced by the territories. In this respect, research work carried out in recent decades has significantly improved the prediction of TCs at all time scales (DeMaria et al. 2014). The advent of coupled ocean–atmosphere models, in particular, constitutes a major step forward in assessing the impact of cyclonic activity at the

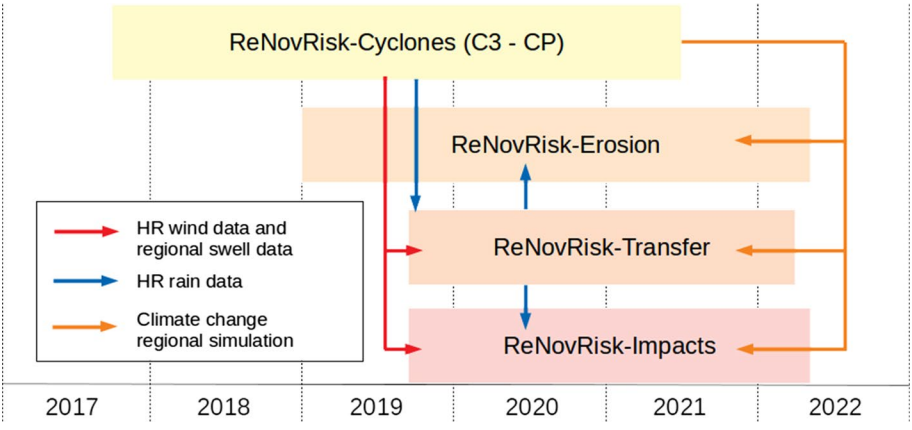

Fig. 1 Scheme of development times of the various ReNovRisk sub-programmes and data-feeding links between them

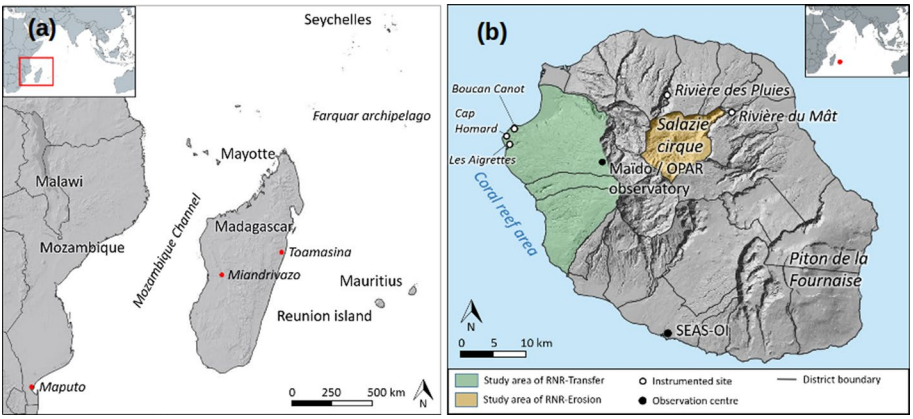

Fig. 2 Geographic area of the ReNovRisk programmes. **a** SWIO domain of ReNovRisk. **b** Reunion Island map and locations cited in the text

regional level (e.g. Eyring et al. 2016; Vitart et al. 2017). Nevertheless, it is commonly agreed that current models do not yet have the technicality and sophistication required to accurately assess the impact of TCs at the local scale.

Coupled numerical weather prediction (NWP) and climate models also require extensive observations to constrain and thoroughly assess the performance of their atmospheric and oceanic components. Because TCs develop, evolve and propagate primarily over oceanic areas, which are generally poorly equipped with conventional observing systems, collecting observations in TC basins can be extremely difficult. Due to the small proportion of land masses and also to the difficulties of sustainably operating observation systems in this poor area, the SWIO is the least instrumented of the six TC basins. Although satellite imagery has now made it possible to track the trajectories and general evolution of TCs all around the world, additional measurements are still urgently needed to study the mechanisms governing the evolution and impacts of low-pressure tropical systems in this particularly active basin.

In this respect, RNR-C has been built along three principal lines:

- An observation component, aimed at providing additional TC observations to calibrate, initialize and evaluate the performance of coupled models in this particularly under-instrumented region;
- A modelling component, aiming at developing a coupled, high-resolution (0.5 km–2 km), ocean–wave–atmosphere modelling system to represent the interactions between a TC and its environment as exhaustively as possible;
- A climate component, aiming at assessing the consequences of climate change on the properties (trajectories, intensity and structure) and potential impacts of tropical cyclones at both local and basin scales.

2.1.1 Observations

The observation component of RNR-C aims to provide accurate observations of TCs and their environments by reinforcing regional- and local-scale observing capabilities in the SWIO. To achieve this objective, RNR-C was built around three approaches.

The first is a conventional and ideally sustainable approach, based on the deployment of regional observation networks and the acquisition of new satellite observations of wind and sea swell in the SWIO. Regarding ground-based observations, a water vapour observing network composed of Ground-based Navigation Satellite System (GNSS) receivers and weather stations was deployed throughout the western part of the basin from November 2017 to September 2020 within the framework of the RNR-C's sub-programme "Indian Ocean GNSS Applications for Meteorology" (IOGA^{4}MET). This important achievement has significantly enhanced water vapour observation capabilities in the SWIO and provides a new tool to thoroughly investigate the water vapour cycle in this area (Lees et al. 2020; Bousquet et al. 2020a).

Regarding space-borne observations, a collaboration with ESA (European Space Agency) and IFREMER (Institut Français de Recherche pour l'Exploitation de la MER) has enabled a unique set of high-resolution (1 km) satellite images of sea surface wind and roughness to be collected from synthetic aperture radars (SAR) deployed onboard the Sentinel 1A/1B satellites of the European Earth Observation programme Copernicus. Throughout 2018 to 2020, SAR data have been acquired on demand (with 48 h notice) for about two-thirds of the TCs that developed in the basin over this period. (About one hundred images were collected, nearly half of which were acquired in the eye-wall regions of TCs and tropical storms.)

The second, an experimental approach, is based on the temporary deployment of various atmospheric and oceanic observation systems at different points in the basin. Several temporary atmospheric and oceanographic observing campaigns have been organized to validate the performance of coupled ocean–wave–atmosphere systems developed within the RNR-C programme (Sect. 2.1.2) the main achievement of which has been the organization of a regional field campaign that took place in various places of the SWIO from January 21 to April 8, 2019. During this field experiment, various sensors were deployed in and around Reunion Island, and in Madagascar, Mozambique, and Mayotte, to sample atmospheric and oceanic environmental conditions during the 2018–2019 TC season. A regional radiosonde network (RS) was deployed in Mayotte (France), Toamasina (Madagascar), and Maputo (Mozambique), enabling 700 soundings to be collected over this 2 ½-month period. Two ocean gliders were launched from Reunion Island to sample the thermodynamic properties of the tropical Indian Ocean up to 500 km from the island. An unmanned airborne system (UAS https://www.boreal-uas.com/), equipped with high-frequency aerosol, wind, and temperature sensors, was deployed for several weeks to measure ocean–atmosphere fluxes and aerosol concentrations in the immediate environment of TCs up to several hundred km from Reunion Island.

The third, an exploratory approach, is based on the deployment and evaluation of new and original methods of investigation to collect oceanic observations in the SWIO from biologging and seismic observations. A particularly original approach, based on biologging technology, has been explored to collect oceanic data from sea turtles equipped with autonomous environmental tags. A first experiment was carried out from January 2019 to September 2020 in the western part of the tropical Indian Ocean, with

the aim of assessing the relevance of low-cost sea turtle borne observations for ocean monitoring and modelling (Bousquet et al. 2020c). Another original approach, based on previous work by Davy et al. (2014, 2016) and Barruol et al. (2016), was also further investigated to evaluate and quantify extreme swell events from microseismic noise measurements recorded by ground-based and underwater seismometers. The analysis of data collected in RNR-C (Rindraharisaona et al. 2020) has demonstrated that terrestrial seismic stations could also be a great alternative for sampling Austral swell events by behaving as ground-based wave gauges.

2.1.2 Mesoscale modelling: improvement of mesoscale numerical models for TC forecasting

An important objective of RNR-C is to design, develop, and evaluate a high-resolution (0.5 km– 2 km) integrated modelling system based on the coupling of state-of-the-art atmosphere, ocean, and wave models. This tool, intended to prefigure fine-scale operational NWP systems to be used by WMO/RSMC Reunion (http://severeweather.wmo.int) in the medium term, will, in particular, investigate the internal physical processes responsible for TC intensification and produce realistic TC simulations over the most densely populated regions of the SWIO basin.

Based on the conceptual model of a tropical cyclone as a Carnot heat engine, the theory formulated by Emanuel (1986, 1988) predicts that the maximum potential intensity depends on the sea surface temperature and the outflow layer air temperature (Bister and Emanuel, 2002). In this context, an ocean–wave–atmosphere (OWA) coupled system has been developed for high-resolution modelling of tropical cyclones in the SWIO (Fig. 3). The coupling between the atmospheric model Meso-NH (http://mesonh.aero.obs-mip.fr/, Lac et al. 2018), the surface model SurfEX (https://www.umr-cnrm.fr/surfex/, Masson

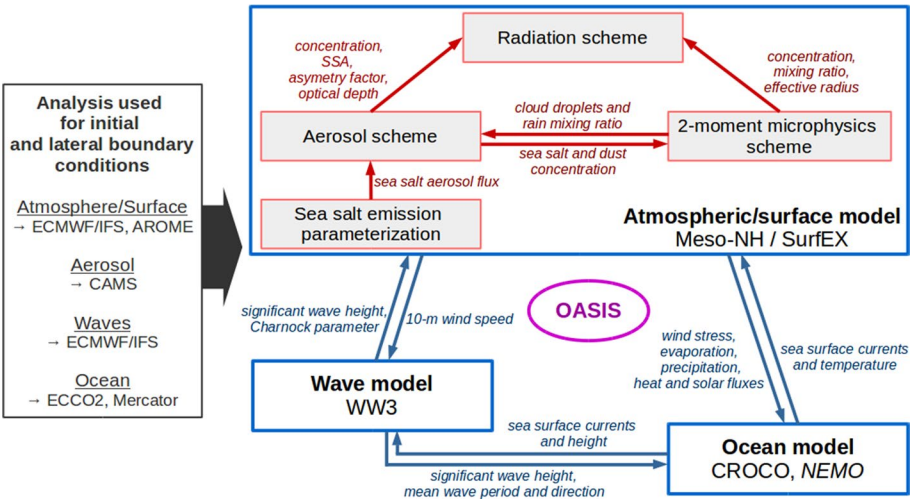

Fig. 3 Schematic diagram of the coupling systems in cyclone numerical modelling. The OWA coupling is shown in blue while the coupling inside the atmosphere/surface model is shown in red. Fields exchanged among the atmospheric, wave, and oceanic models are shown in blue italics; they are exchanged at intervals defined by the user (typically ~ 10 min). Fields exchanged among the atmospheric schemes are shown in red italics; they are exchanged at each time step

et al. 2013), the wave model WaveWatch III (http://polar.ncep.noaa.gov/waves/wavewatch/) and the ocean model CROCO (http://www.croco-ocean.orgref) was realized through the OASIS coupler (https://portal.enes.org/oasis, Craig et al. 2017) as described by Voldoire et al. (2017) and Pianezze et al. (2018). This coupled system is particularly innovative since it enables the user to represent (i) the air–sea interactions, which have long been recognized as a key issue in improving the accuracy of tropical cyclone intensity (e.g. Rotunno and Emanuel, 1987), (ii) the swell generated by the strong winds, and (iii) the sea salt aerosol emissions induced by the combined effects of strong winds and waves (Andreas et al. 1995). In non-polluted environments, these sea salt aerosols are the main source of condensation nuclei for cloud formation. A parameterization of such aerosol emission as a function of atmospheric, oceanic, and wave parameters (Ovadnevaite et al. 2014) has been introduced in the atmospheric/surface model. Once emitted, these aerosols are integrated in the ORILAM aerosol scheme (Tulet et al. 2005): they are transported by advection and turbulence and can be lost by sedimentation, and dry or wet deposition. The aerosol scheme was then coupled with the two-moment bulk microphysics scheme LIMA (Vié et al. 2016) as described in Hoarau et al. (2018a). Since cloud–radiation interactions are suspected to influence the track (Fovell et al. 2016), the structure (Bu et al. 2014) and the intensity (Trabing et al. 2019) of a tropical cyclone, specific developments on the secondary formation, and habits of ice crystals (Hoarau et al. 2018b) in the LIMA microphysics scheme are in progress. This will enable a better description of the ice water content, the ice crystal effective radius and the ice crystal shape, which are used as input for the radiation scheme. Attention has also been paid to initial and lateral boundary conditions for each component (atmosphere, surface, aerosol, wave and ocean) of the coupled system (see the box on the left in Fig. 3). This coupled system can be viewed as a prototype for the French operational model AROME. It has been run on several tropical cyclones (Bejisa, 2014; Fantala, 2016; Berguitta, 2018; Idai, 2019) to produce high-resolution precipitation, wind and wave fields all over the SWIO, and deliver some of these fields to the other sub-programmes.

2.1.3 Climate modelling

While it is generally accepted that global warming will have a significant impact on ocean surface temperatures, which is a factor favouring the development of TCs, no one really knows how the other ingredients involved in the formation of tropical low-pressure systems will evolve in the future. While disaster scenarios suggest an increase in intense events, some scenarios also suggest a "benevolent nature" that could counteract this pessimistic trend. In this respect, a key objective of RNR-C is to assess the consequences of climate change on the properties and potential impacts of tropical cyclones in the SWIO basin. The experimental strategy is based on two complementary approaches: (i) the use of high-resolution global and regional climate simulations to estimate the evolution of cyclonic activity at basin scale (changes in TC trajectory, intensity and structure; impact on water resources) and (ii) the use of high-resolution mesoscale coupled simulations to assess the potential impact of climate change on the structure and the impacts of TC in specific target areas such as Reunion Island.

To address this issue, high-resolution (~20 km–25 km) global climate simulations found with the French climate model ARPEGE-Climat (https://www.umr-cnrm.fr/spip.php?article124&lang=en) have been run to assess the impact of climate change on the frequency, distribution and, to a lesser extent, intensity of future tropical cyclones (Cattiaux et al. 2020). Higher-resolution simulations have also been carried out using the limited-area

climate model ALADIN-Climat and the integrated OWA model developed in the programme (Fig. 3) to analyse the response of TC to climate change in terms of structural development and determine whether changes in storm activity and/or structure will pose an additional threat to coastal areas and islands of the SWIO basin in the future (Thompson et al. submitted). The first results obtained from the analysis of the various simulations carried out in the programme are presented in Sect. 3.5.

2.2 ReNovRisk-erosion (RNR-E)

Among the impacts of cyclones landing on Reunion Island, hydrological floods, sediment fluxes and erosional processes are causes of major concern to population and infrastructures. The hydrological regime of the island's rivers stands out for the coexistence of several major parameters that predispose it to extreme vulnerability. Holding almost all the world records for rainfall between 12 h (1170 mm) and 15 days (6083 mm), the island presents a very marked relief with a peak at 3,069 m, exceptional escarpments up to 1500 m in height and having an average slope of over 70°, and very steep natural valleys and cirques. As a result, all the processes that can lead to erosion and ground movements are particularly active in Reunion Island.

The objective of the sub-programme RNR-E falls within this major issue regarding forecasting of and protection against torrential floods. Liébault et al. (2010) point out that the characterization of erosion and sediment transport in Reunion Island rivers requires better knowledge of the hydrological-hydraulic and geomorphological processes that control the production and transfer of liquid and solid flows.

To meet this target, RNR-E involves the monitoring and data acquisition at various scales of two representative hydrological catchment areas on Reunion Island: Salazie cirque and Rivière des pluies (Fig. 2b). New instrumentation has been set up in the aim of analysing and quantifying the interactions between upstream and downstream in the following processes:

- Formation of the sedimentary stock: this is linked to erosion phenomena in the upstream parts of the catchment areas and to gravity destabilization (in particular rampart collapses and landslides). GNSS, a network of geodetic markers, LiDAR and seismic surveys are being implemented on the six major large-scale landslides in the Salazie cirque and in the Rivière des Pluies watershed. We are also carrying out hydrological, hydrogeological and geochemical monitoring of groundwater and surface water at the level of these landslides. In addition, the structure from motion technique has been applied using historical aerial images, image correlation techniques and SAR interferometry to characterize landslide dynamics.
- Flow processes: completing the hydrological monitoring equipment of the experimental catchment "La Rivière des Pluies", which is part of the French OZCAR network (https://www.ozcar-ri.org/observatories/the-network/), RNR-E proposes to detail the variability of the contribution of tributaries to the flash flood processes. Specific photogrammetric discharge monitoring stations are used in order to document an accurate rainfall–runoff model (Stumpf et al. 2016).
- Bedload transport: as direct measurements of the bedload transport are extremely difficult to make during a tropical cyclone, RNE-E uses the high-frequency seismic noise generated by the rivers as a proxy for the sediment transport. Eleven broadband seismometers have been deployed along two rivers, both located in the northern side of the

island (Rivière des Pluies and Rivière du Mât, Fig. 2b), in the framework of the "Rivière des Pluies" temporary seismic network (Fontaine et al. 2015). This has allowed us to analyse the spatial and temporal variations of the seismic noise along these rivers with respect to the rainfall and hydrological data, and to characterize the bedload variations during tropical storms and cyclones (Gonzalez et al. 2017; Gonzalez 2019; Gonzalez et al. submitted). A very good correlation was obtained between the seismic noise amplitude and the water level during the river flood related to TC Dumazile in March 2018 (Gonzalez 2019; Gonzalez et al. submitted). Preliminary results show that the amplitude of the high-frequency seismic signal (> 1 Hz) recorded at the seismometers may be used as a proxy for the water level during a cyclone. Spectral and polarization analyses of seismic data were also used in order to decipher the seismic signature of water flow and bedload transport.

Firstly, it was shown that the behaviour of landslides can be modelled by inverse models with a bimodal transfer function using a Gaussian-exponential impulse response, linked to the rain and piezometric level (Belle et al. 2014). Then, the recharge of the large Grand Ilet landslide (350 Mm^3) in the humid tropical season was characterized through a robust, multidisciplinary hydrological approach, notably comprising a precise water budget of the landslide. It appears that surface processes play a major role in the landslide recharge regime (Belle et al. 2018).

Then, landslide displacement mapping based on ALOS-2/PALSAR-2 data using image correlation techniques and SAR interferometry was applied to the Hell-Bourg landslide (Raucoules et al. 2018). The capability of space-borne high-resolution L-band synthetic aperture radar (SAR) images (ALOS-2/PALSAR2 data in StripMap SM1 mode) for deriving and mapping two components of the deformation of slow landslides has been investigated. The deformation was characterized on the basis of sub-pixel correlation offset tracking techniques and differential SAR interferometry. On the Hell-Bourg landslide (Fig. 2b, with displacements up to about 1 m $year^{-1}$), the deformation maps produced performed significantly better than the C-band or lower-resolution SAR data used in previous studies. A comparison was carried out with GNSS data acquired on the test site. Even with a reduced image set (seven acquisitions), detailed deformation maps and information on deformation evolution during 2014–2016 could be generated.

Finally, RNR-E has implemented a new methodology based on structure-from-motion processing of archive aerial photographs to quantify geomorphological changes in Reunion Island since 1978 (Rault et al. 2020). Photographic archives indeed hold a decades-long 3D history and, for the first time, our measurements reveal the cumulated signature of landslides on the Cirque de Salazie from 13 cyclones over the 37 years investigated. Such an approach demonstrates that the structure-from-motion technique is a game changer for landslide risk mitigation planning.

Most of the acquisition of the data presented above is still ongoing (as of September 2020) and is ready for the next cyclonic event in Reunion Island.

2.3 ReNovRisk-transfer (RNR-T)

RNR-T focuses specifically on the study of cyclonic hazard transfer in natural environments. It focuses on the natural risks associated with cyclones landing on Reunion Island and more specifically on the western micro-region, taking its workshop area as the Maïdo massif, the coastal strip between Saint-Paul and Saint-Leu, the back reef lagoon and the

open ocean, depending on the position along the coast (green area in Fig. 2b). The general objective is to analyse how cyclonic hazards are transferred between the natural environments of the atmosphere, the hydrosphere, the littoral zone and the open ocean. With regard to the transfer from the atmosphere to the hydrosphere and the coastline, the atmospheric hazards are the wind gusts and precipitation associated with cyclonic events. These hazards depend on many factors intrinsic to the cyclone and other factors in relation with the landfall area. Cyclonic winds are, by nature, the most intense in the upper reaches of Reunion Island, an area where the most intense cyclonic precipitation is generally also found. The scientific questions associated with these themes arise at the interfaces of the natural environments.

Between the atmosphere and the hydrosphere, the challenge concerns the quality of the precipitation data that are delivered to hydrologists to initialize hydrological models. Whether the issue is the rainfall observations or the forecasts by numerical models, the difficulties lie in the validation of the quality of the data. The spatial representativeness of rainfall and wind observations is a key factor for studying natural hazards, especially in the complex topographical context of Reunion Island. These scientific questions are being attacked by meteorological observations at the OPAR observatory (https://opar.univ-reunion.fr/) using new data fusion and numerical modelling methodologies to produce high-resolution rain and wind data of landfalling TCs over Reunion Island, with a focus on the Maïdo massif.

For this purpose, a numerical modelling method to produce low-cost high-resolution wind fields of landfalling TCs has been developed. To produce wind fields consistent with both the position and intensity of the system, the large-scale environment and the topography of the targeted region, the Meso-NH atmospheric model was implemented with Holland's parametric approach (Holland 1980) coupled with the use of meteorological analysis from the IFS (Integrated Forecasting System) model of ECMWF (European Centre for Medium-Range Weather Forecasts). The parameters used in the Holland formulation are deduced from the RSMC Reunion Island best-track. This so-called bogus method was set up within the framework of the SPICy programme (Système de Prévision des Inondations en contexte Cyclonique, http://spicy.brgm.fr/fr) and tested on 5 historical cyclones that affected Reunion Island (Bejisa, Dumile, Felleng, Gamède and Dina). The structure reproduced was shown to be realistic as long as the information on the radius of the maximum winds injected into the bogus was relevant. The wind fields reconstructed by the bogus method showed good agreement with in situ observations as soon as the orography of the island was well reproduced. This method was deployed in the framework of the ReNovRisk programme (Vérèmes 2020, Technical Report). To date, high-resolution wind fields of 6 tropical cyclones at landfall on Madagascar and Reunion Island have been produced. 10 m wind gusts were provided at a horizontal resolution of 500 m on Reunion Island for Dina (2002), Berguitta (2018) and Bejisa (2014), and on Madagascar for Enawo (2017). A horizontal resolution of 2 km was used on Madagascar for Gafilo (2004) and Ava (2018). This approach enables us to produce high-resolution wind fields at low numerical cost. It should be noted that this tool does not permit the precipitation fields to be produced since the rainbands are not reproduced by the bogus method.

Additionally, the operational product ANTILOPE (ANalyse par spaTIaLisation hOraire des PrEcipitations) archived by the French meteorological office (Météo-France) has been implemented over Reunion Island. ANTILOPE estimates the quantity of rainfall at the scale of a 1 km^2-grid from radar data corrected by rainfall data (Laurantin 2008). The archived product is calculated for a 1-h time step. It is a hybrid product of the PANTHERE quantitative precipitation estimate (QPE) (Parent du Châtelet et al. 2005) and a kriging

interpolation of the rain gauges available at the time of QPE (Pauthier et al. 2016). The variation of the radar reflectivity over the hour is analysed for each pixel of 1 km^2 and in steps of 5 min. This variation automatically associates a fraction of the current hour with a convective rainfall (between 0 and 60 min) and its complementary fraction to a stratiform rainfall. The stratiform part is obtained by kriging the large-scale rainfall values, whereas the convective part is obtained by detecting cells on the radar images and is corrected using the convective accumulations of the rain gauges located under these cells. The ANTILOPE data were not produced and archived by Météo-France until 2016. However, for Reunion Island, the PANTHERE rain data have been available since the end of 2013, so a reprocessing of the ANTILOPE data over the 2014–2019 period for Reunion Island is possible. ANTILOPE almost fully corrects the underestimation of the precipitation obtained from PANTHERE (Fig. 4). Within the framework of RNR-T, an external service was therefore entrusted to Météo-France to reprocess the entire database for the Reunion Island area. The 15-min time-step ANTILOPE dataset has been generated for the 2014–2019 period with a horizontal resolution of 1 km^2. It provides a view not only of cyclonic rains but of all rainfall on Reunion Island and will thus make it possible to assess the exceptional nature of past or future events. The ANTILOPE database is also expected to provide input data for econometric models developed by RNR-I.

Along the western slopes of the Maïdo massif, the challenge in the hydrosphere stems from a lack of knowledge of the behaviour of temporary ravines of the Maïdo massif, in particular their disconnection from the underground reservoirs and their very large infiltration capacities at the beginning of the rainy season. Time series of stream flows in these ravines are very sparse and most often uncorrelated with the simultaneous availability of good rainfall series. RNR-T will attack these obstacles, firstly by setting up hydrological instrumentation along two ravines in almost ungauged catchments and, secondly, by using a semi-distributed rainfall–runoff model (Rojas-Serna et al. 2016; De Lavenne et al. 2019). This model has fine spatial resolution (square kilometre) and hourly time steps, suited to the nonlinear behaviour of this type of ravines, and is sequentially calibrated considering

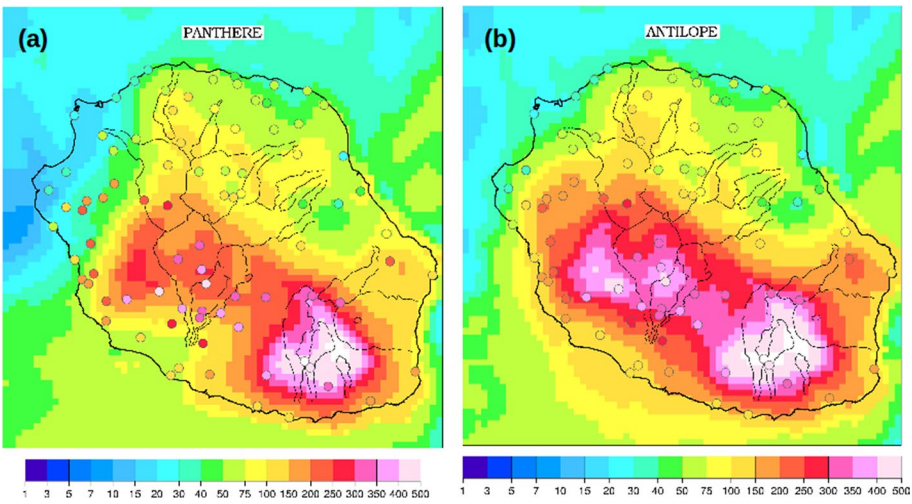

Fig. 4 Cumulative rainfall (mm.day-1) observed on January 1, 2018 during TC Beguitta with PANTHERE **a** and ANTILOPE **b**. Rain gauge data are superimposed (coloured circles)

the observations available at the outlet of the catchment and at different gauging points inside the catchment (De Lavenne et al. 2019).

The Maïdo watershed is characterized on the sea side by the largest fringing reef of Reunion Island (400 m wide). Although the contributions of the watershed are weak on a yearly scale, allowing the development of the reef life, in a cyclonic context the forcing of the watershed, is not negligible. The inputs of fresh water loaded with suspension and nutrients modify the reef environment and can alter the calcification and therefore the growth of the coral. Oceanic forcings (swell) on the reef barrier remove pieces of coral, which can feed the beaches with coral debris. Water masses that submerge the reef barrier and pass through the reef system are the vector of a strong littoral drift. The instrumented site of "La Passe de l'Hermitage" (coral reef area on Fig. 2b) has been set up to quantify the processes and impacts of cyclonic events. The interdisciplinary scientific team in charge of this site is developing tools and indicators to observe, monitor and model the impacts of climate change in the coastal reef zone, and the possible synergy with local anthropogenic pressures. The measurement activity includes (1) monitoring global and local anthropogenic pressures (ocean acidification, freshwater groundwater flow, beach frequentation), and (2) monitoring indicators of beach morphological dynamics and loss of resistance and/or resilience (reproduction and recruitment of scleractinian corals and millepores, carbonate balance), and mapping the trajectories of benthic communities in response to disturbances. These activities are partially approved at the national or international level (SNO Dynalit; https://www.dynalit.fr/).

2.4 ReNovRisk-impacts (RNR-I)

The main goal of RNR-I is to assess both the economic vulnerability and the potential economic impacts of cyclones. Such evaluations are intended to serve as decision support tools in policy- and decision-making.

Among the impacts of natural hazards (see, for example Hallegate (2014)), RNR-I will pay special attention to two distinct effects. On the one hand, immediate direct effects, namely the direct monetary costs of destruction/reconstruction due to the damage caused by a TC event, will be considered. On the other hand, indirect long-term effects (belated observable effects caused by the consequences of a TC over the territory) will be studied focusing on i) the macroeconomic repercussions of the aforementioned damage throughout the territory (cross-sectoral effects) and ii) the consequences on socio-economic determinants (e.g. fertility or education).

For direct effects, RNR-I seeks to develop a general protocol largely based on spatialized analysis, which can include bottom-up (Reunion Island) as well as top-down (Madagascar) cases. At the core of this protocol is the idea that impacts are a combination of hazard, exposure and vulnerability. Regarding hazard, a TC presents particularities that should be taken into account, as characteristic rainfall and high-speed winds of TCs (multi hazard-inputs) can induce storm surges, flooding events and landslides (cascading hazard outputs), which are also likely to significantly amplify the vulnerability of the territory. Intersecting hazard maps with land-cover information, RNR-I produces exposure maps (of entities likely to be impacted by the hazards-output). Building from these maps, we will focus on the physical and economic dimensions of vulnerability evaluated by means of damage functions. The physical vulnerability approaches the variable degrees of individual damage that, e.g. buildings, infrastructures or crops, suffer depending on the intensity of the hazard

(confirmed by remote sensing). The economic valuation of the level of destruction, linked to the value of the land use, determines the economic vulnerability.

For the characterization of cascading output hazard, monitoring the spatial footprint of the TC impacts by remote sensing offers great potential for assessing the extent of impacted areas. For this purpose, RNR-I has developed two automated processing flows, based on high spatial resolution optical and radar satellite data (10 m), that detect changes between a reference image before the cyclone and post-event images. These two analyses are complementary. Changes detected with Sentinel-1 data, based on the normalized difference ratio, allows the extent of flooded areas to be monitored as close as possible to the cyclone event (Alexandre et al. 2020). Changes detected with Sentinel-2 data, based on the use of change vector analysis (CVA) (Mouquet et al. 2020), which has shown its potential for monitoring changes in surface states (Hussain et al. 2013), allow a better characterization of land-cover change over longer time periods. Various events in the SWIO have been processed, and the results have been made available to the public.

For indirect effects, the negative impacts are not as obvious, especially because propagation mechanisms within socio-economic dimensions remain mostly undisclosed. RNR-I tackles this issue through two complementary approaches. We first rely on modern econometric techniques (Dell et al. 2014 or Camargo and Hsiang, 2016) together with the opportunity of merging geolocated data on the magnitude of TCs, and also on both economic and social features. The econometric strategy enables us to focus on how households reorganize their lives in the aftermath of TCs. One innovation of RNR-I is to focus on the causal effect of TCs on birthrate. The second approach undertakes the construction of theoretical models (CGE), accounting for the interdependence among economic agents, to explain the transmission channels through which the indirect effects take place (Narayan (2003) or Botzen et al. (2019)).

The data of RNR-C and RNR-T will be used by RNR-I for direct comparisons with the outputs of the system detecting changes in satellite images following the passage of a tropical cyclone. Furthermore, the simulated wind fields will also be used by RNR-I as output-hazard data for the development of either simulation models—computational laboratories devoted to the ex-ante evaluation of shocks—or econometric models—statistical models based on ex-post data in the aim of uncovering relations between relevant variables—to evaluate the potential socio-economic impact of cyclones (see Sects. 3.1 and 3.4). In the particular case of TC Enawo, the cross-analysis of the modelled wind field with the results of the change detection algorithms on Sentinel 2 satellite images shows good correlations between the maximum winds and the decrease in vegetation cover over a hundred kilometres around the landfall point, despite the difference in resolution and the presence of numerous clouds at this period (not shown).

3 Presentation of cross-disciplinary results

3.1 Floods following TC Ava in the Miandrivazo region

Coming from the north-east of the island, TC Ava landed on 5 January 2018 near the city of Toamasina on the east coast of Madagascar, with sustained winds of more than 150 km h^{-1}. Overall, the cyclone severely hit and caused heavy rainfall throughout the central part of the country and particularly in the studied region of Miandrivazo (Fig. 2a). Rainfall image maps computed from RNR-C meteorological models showed that TC Ava

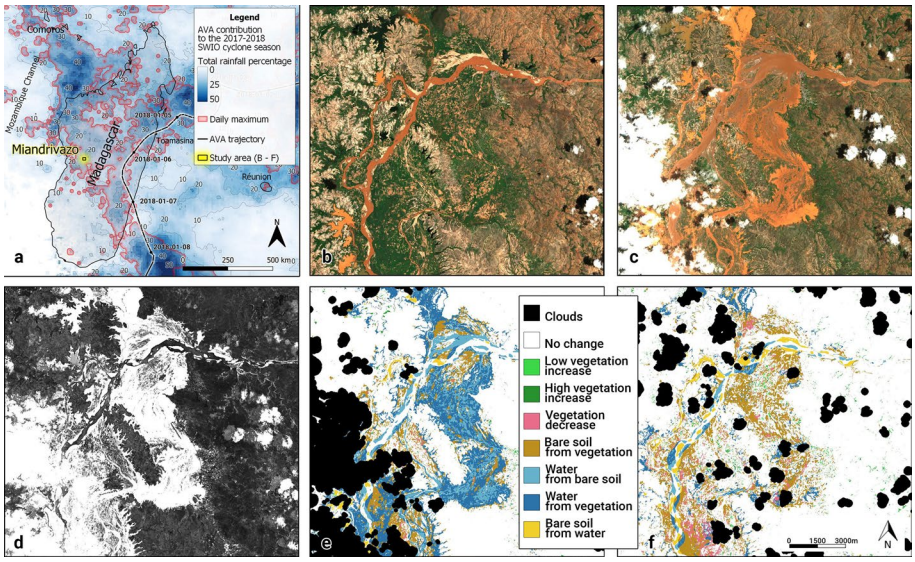

Fig. 5 Detection of changes between two remote-sensed images associated with TC Ava. **a** Location map of the Miandrivazo study site in Madagascar and meteorological conditions during TC Ava. **b** Sentinel-2 imagery of the region before the cyclone (25/12/2017) and **c** after cyclone Ava (09/01/2018). **d** Magnitude of changes between images (b) and (c) (the lighter the shade, the greater the change). **e** Classification of the main categories of changes just after the cyclone impact (09/01/2018) and **f** ten days later (19/01/2018)

brought about 20% of the total annual rains and reached the maximum daily precipitation for the whole 2017–2018 cyclone season in this area (Fig. 5a).

With the image of 25 December 2017 as a reference, we used the CVA algorithm to highlight areas of greatest change and compute classification maps of the impacts on two post-event images, 9 and 19 January 2018, respectively, 4 and 14 days after the event (Fig. 5b and c).

The results show a first rapid flooding of the entire floodplain, covering agricultural and forest plots, but sparing buildings and urban areas located on higher ground (day + 4, Fig. 5d and e). Two weeks after the event, most of the flooded areas were replaced by bare wet soils, mainly affecting the agricultural parcels, which suffered strong decreases in crop cover. The main riverbed was deeply and durably modified, with the appearance of sand-banks and new water bodies (Fig. 5f).

3.2 Cyclonic heavy precipitations on landslides

A forced atmospheric high-resolution (500 m) simulation of TC Bejisa initialized and coupled at the lateral boundaries by the ocean–wave–atmosphere system (Meso-NH-OVA described previously with a 2 km resolution) has been carried out in order to obtain higher-resolution wind and rainfall maps over Reunion Island. The 24-h cumulative rainfall on 1 January 2014 during TC Bejisa shows three zones with cumulative rainfall greater than 250 mm in both the observations and the simulation (Fig. 6). The rainfall observations are a merged product of rain gauges and radar data given by the ANTILOPE QPE product. The zone of heavy rainfall in the centre of the island is relatively well reproduced by the model,

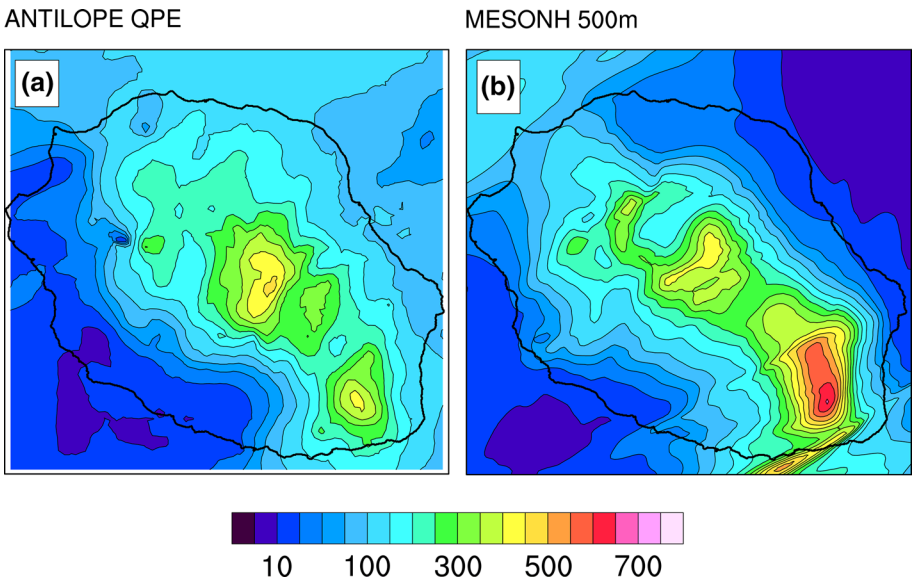

Fig. 6 Cumulative rainfall over 24 h for the day of January 1, 2014 (mm) given by ANTILOPE QPE (radar and rain gauge observations, (**a**) and modelled by Meso-NH with a horizontal resolution of 500 m (**b**)

although the simulation tends to give slightly higher maximum values (~500 mm) than the merged data (~450 mm). In the simulation, the maximum rainfall is located on the south-eastern flank of Piton de la Fournaise (Fig. 2b) with values greater than 700 mm, whereas they barely reach 400 mm in the observations. This tendency of the models to overestimate rainfall on the south-east flank of the volcano has been found in other simulations of intense precipitation events. It should be noted, however, that the density of rain gauges is quite low and that radar acquisition in this area is partially masked by the orography. The third, northernmost, zone of maximum cumulative rainfall is overestimated by the model. While the cumulative rainfall is relatively well represented by the model on the west coast of the island, with values between 10 and 100 mm, the model tends to underestimate the cumulative rainfall over the north-east and east. This may be due to the slight shift of the modelled TC to the west compared to observations. Even though the rainfall restitution is not perfect, and taking into account the uncertainties in the production of an observed 2D rainfall field (especially in areas with low coverage in observations such as the south-eastern flank of the volcano), using a resolution of 500 m significantly improves the spatial distribution of rainfall (not shown).

During TC Bejisa (January 2014), beyond many small "normal landslides", a significant one (1.1 million m^3) occurred in the centre of Reunion Island in the Salazie area (Fig. 2b and Fig. 7). After regular field observations, its volume was calculated by comparing two high-resolution DEM (LiDAR surveys). This landslide resulted in the accumulation of a large amount of various materials in the "Roche à Jacquot river" bed (Salazie cirque), most likely creating a temporary dam in the river. The dam vanished rapidly during Bejisa because of the strong river flow (a few tens of $m^3\ s^{-1}$). Fortunately, neither the landslide nor the rupture of the dam had an impact on infrastructure or people.

In the next step, rainfall data produced by ANTILOPE will be used to estimate the slope instabilities. Groundwater is one of the multiple and various factors that significantly

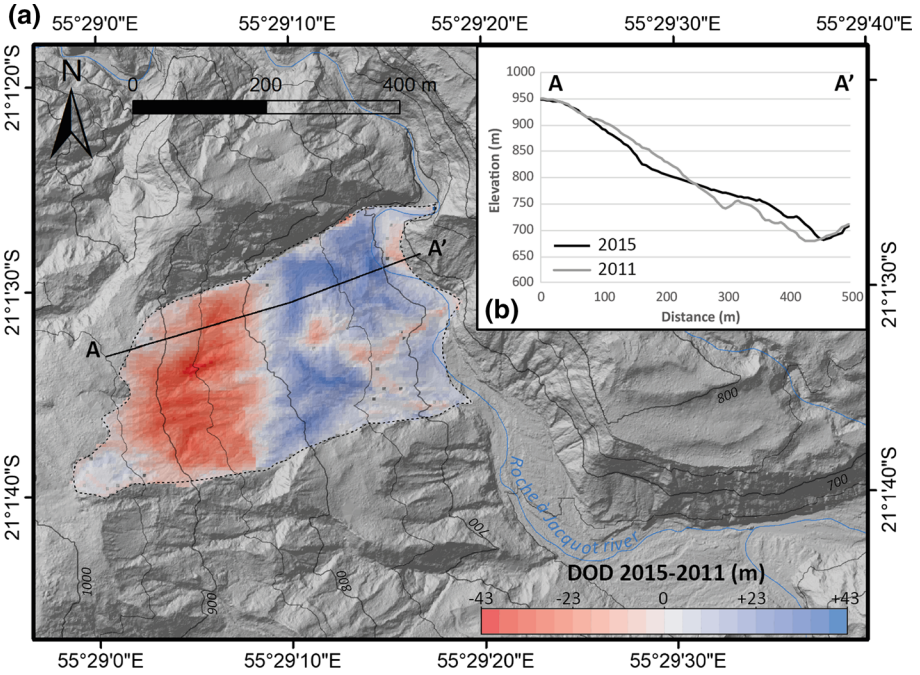

Fig. 7 1.1 Mm^3 landslide triggered by the cyclone Bejisa in 2014 in Salazie. (a) DEMs of Difference (DOD) at 5 m resolution in the area affected by the landslide, surrounded by the dotted line; the red (erosion) and blue (accumulation) zones reveal major topographic changes between 2011 and 2015 (acquisition years of the DEMs). The black line A–A' marks the ends of the 2011 and 2015 topographic profiles presented in (**b**) showing clear mass transfer

influence landslide displacement. A rise in water tables during aquifer recharge (e.g. after rainfalls) increases hydrostatic pressure in the media, which tends to decrease the landslide shear strength and cause the landslide to accelerate (Iverson and Major 1987; Baum and Reid 1992; Van Asch et al. 1999; Coe et al. 2003; Cappa et al. 2004; Corominas et al. 2005; Schulz et al. 2009).

The prediction of the movement pattern of landslides is assessed using physically based numerical modelling approaches (Corominas et al. 2005; Malet et al. 2005; Tacher et al. 2005; van Asch et al. 2007; Fernández-Merodo et al. 2012) or inverse numerical modelling that combines both numerical approaches and observations (Belle et al. 2014; Bernardie et al. 2015; Vallet et al. 2015). For both techniques, accurate spatial and temporal rainfall data are required.

3.3 Cyclonic swell impact on beach profile morphology

The ReNovRisk programme seeks to relate the evolution and distribution of cyclonic wave heights to the evolution of the coastline and the coastal sedimentary stock on Reunion Island. The first exploratory study was based on TC Bejisa.

The swell field was extracted from a simulation at 2 km horizontal resolution using the coupled ocean–waves–atmosphere system (CROCO, WW3 and Meso-NH) (Pianezze et al. 2018). The significant wave height and direction are shown in Fig. 8. On 1 January

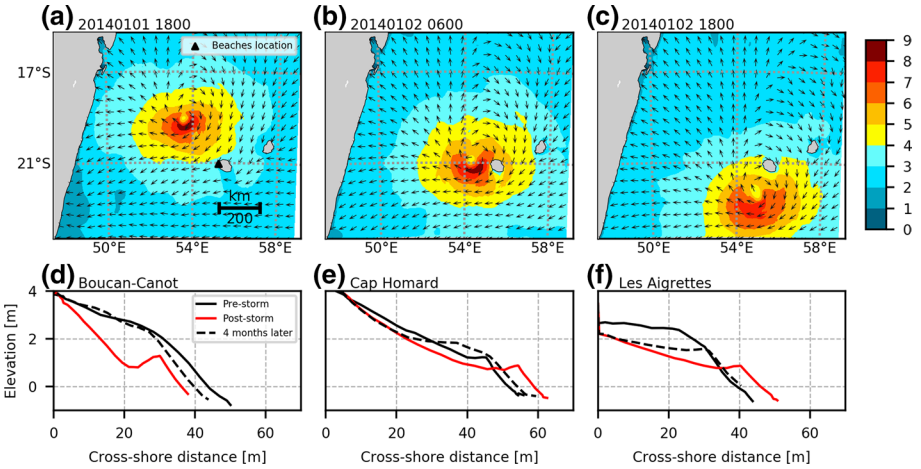

Fig. 8 Top: Significant wave height and direction simulated by Meso-NH-WW3-CrOCO during TC Bejisa. **a** 01 January 2014 at 18 UTC, **b** 02 January 2014 at 06 UTC, and **c** 02 January, 2014 at 18 UTC (Based on Pianezze et al. 2018). Bottom: Morphosedimentary evolution of beach topographic profiles caused by cyclone Bejisa at three sites:**d** Boucan Canot, **e** Cap Homard and **f** Les Aigrettes. Pre-storm topographic profiles (black lines) correspond to the date of 14 December 2013, post-storm (red lines)–17 January 2014 and the black dotted line corresponds to 4 months after Bejisa, that is, to 27 May 2014

at 18 UTC (Fig. 8a), the system was located north-west of Reunion Island and moving southwards, the maximum significant wave height, between 8 and 9 m, being concentrated under the wall of the system. When it passed closest to the island on 2 January at 06 UTC (Fig. 8b), the whole coastline was exposed to waves, and the maximum significant wave height of the cyclone was around 9 m. After Bejisa had passed close to the island's coasts, the south and west facades were still affected by strong swell as the wave fields also propagated northwards (Fig. 8c).

At the same time, within the framework of DYNALIT, the seasonal and paroxysmal morphosedimentary dynamics of beaches were monitored (Mahabot et al. 2017a, b) along three cross-shore profiles of the carbonate sandy beaches that were impacted by the cyclonic swell of TC Béjisa: "Boucan Canot", "Cap Homard" and "Les Aigrettes" (location on Fig. 2b).

Close to these three beaches, the temporal evolution of the cyclonic swell was characterized by a coupled simulation. The simulated significant wave height exceeded 3 m for 37 h from 1 January at 19 UTC to 3 January at 9 UTC. Since this swell was directly produced under the TC, as the TC passed along Reunion Island, the wave direction varied from south to east, affecting these beaches differently. To assess the impact of TC Bejisa on these three beaches, measurements by Differential Global Positioning System were made one month before the cyclone, two weeks after and 4 months after the cyclone. Profiles were established on a radial between the foreshore and backshore. The profile of Boucan Canot (Fig. 8d) presents the main morphological and volumetric change induced by Bejisa. The toe of beach retreat attained 7.5 m and very significant erosion can be observed along the profile, which reaches a thickness of 2 m between 20 and 25 m cross-shore distance. Along the profile, the volume change rate attained -42.53 ± 1.6 m^3. Four months after Bejisa, during fair-weather conditions, waves slowly carried material back on shore to rebuild–more or less–the original profile. However, the lower foreshore still retains the

after effects of the cyclonic swell and the head of the beach profile also shows a slight loss of sediment thickness, which can be expected to be perennial as there is no more dune recharge on this built-up coastline. After Bejisa, the Cap Homard (Fig. 8e) profile essentially shows a displacement of the beach berm by about 10 m, resulting in an advance of the beach profile of about + 7.2 m. In addition, the whole profile underwent a decrease in sedimentary thickness of about 40 cm on average. In addition to this transfer between the backshore and foreshore, the cumulative sediment loss was -6.76 ± 2.21 m^3. Four months later, the beach was rebuilt with a convex berm that was larger than before Bejisa hit. Finally, the Les Aigrettes profile (Fig. 8f) shows a sediment transfer from the backshore to the foreshore and the nearshore, resulting in an advance of the beach profile by about + 6.7 m. However, this advance was the result of the transfer from the backshore/foreshore to the nearshore zone. The volume change of -23.42 ± 1.71 m^3 after Bejisa is a good indicator of the lowering of the beach profile. Four months later, the profile had not recovered its initial morphology. Although beach recovery from severe storms has been shown to spread over years to decades (Dodet et al. 2018), in Reunion Island, on coral reef beaches, no long-term reconstruction of beach profiles has been demonstrated (Mahabot et al. 2017a, b).

3.4 Integration of simulated wind fields in the evaluation of direct economic impacts

Wind-induced physical damage to buildings and infrastructures can be very severe and increase their vulnerability—and the vulnerability of the assets they may contain—to TC induced hazards, such as floods. The identification of such damage, and its consequences in the socio-economic fabric, is therefore essential for the evaluation and quantification of TC impacts (Tamura 2009; Camargo and Hsiang 2015).

The simulations of high-resolution wind fields produced by ReNovRisk using the Bogus method (Sect. 3.2), given their dynamic character (output every 15 min), can be used to finely identify entities exposed to potentially damaging winds.

In the computational models for the ex-ante evaluation of economic impacts under development in RNR-I, the utilization of the high-resolution wind fields simulated enables both the entities exposed and the duration of the exposure to be identified. In turn, this thorough identification of exposed entities should allow fine estimations to be made of potential damage to buildings, infrastructures and plots. Figure 9 illustrates the potential of the simulated high-resolution wind fields in the analysis of exposure. The figure represents three snapshots of the simulation of cyclone Bejisa, over a layer of urban land use composed of buildings and infrastructures, in which the changes in wind speed can be appreciated as the cyclone moves southward (wind speeds represented have been limited to those that can cause damage, i.e. those higher than ~ 25 m s^{-1} (Tamura 2009)). As can be appreciated, the identification of entities exposed to damaging winds, together with an estimation of the duration of the exposition, is fairly straightforward with this method and highly valuable for a fine evaluation of potential direct damage.

3.5 Cyclonic impact on human reproduction in Madagascar

Estimated wind fields generated by TCs can be used within an econometric framework to investigate questions related to their impacts on social or economic characteristics (Dell et al. (2014), Hsiang and Jina (2014) or Strobl (2012)). As an example of TC social impact, RNR-I studies whether TCs may change parents' decisions

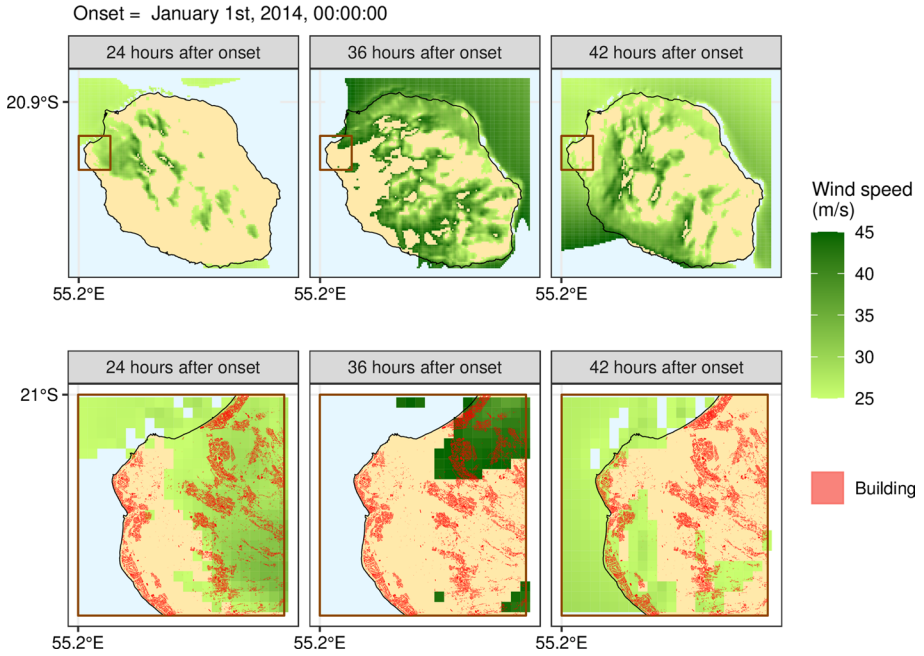

Fig. 9 Example of a GIS-based method for the evaluation of the dynamic exposure. Top from left to right: evolution of damaging wind fields (speed equal to or higher than 25 m s^{-1}) over Reunion Island taken from the simulation of TC Bejisa. Bottom from left to right: close-up maps (15 km × 15 km) enabling the identification of buildings and infrastructures exposed (location and duration) to damaging winds

about having children in Madagascar. This is being done by using geolocated microdata from the Malagasy Demographic and Health Survey, together with wind field data generated by tropical cyclones hitting Madagascar during the 1985–2009 period (Geiger et al. 2017). Merging geolocated data with the full fertility history of the women interviewed enables a unique dataset to be constructed, potentially emphasizing links between births and the mothers' TC experiences. RNR-I then applies panel econometric techniques, exploiting year-to-year variations in exposure to TCs, to estimate the causal effect of TCs on mothers' likelihood of giving birth. The main result of this study is that, on average and all other things being equal, exposure to wind speeds of 27.8 m s^{-1} (approximately 100 km h^{-1}) implies a total fall in the probability of giving birth of 25.6 points in the current year, together with a further decline of 5.9 and 2.0 points, respectively, one and two years after being exposed. Alternative estimations of the empirical model show that the adverse effect of TC exposure on the number of births is persistent. The estimated effect is shown to be robust to many alternative specifications of the econometric model. This new empirical evidence is consistent with economic mechanisms suggesting that TC exposure is perceived as an adverse shock—generating uncertainties in many aspects of daily life (loss of income, crops, livelihood)—that leads couples to postpone their decision to have children.

3.6 Evolution of TCs in the SWIO in the context of climate change

The evolution of tropical cyclones (frequency, intensity, trajectory, seasonality, etc.) in a warmer climate remains largely uncertain: the theory is poorly known, the series of observations are heterogeneous in time and space, and most of the multi-model climate projections available so far are too poorly resolved (100 km or more) to properly represent these phenomena. Nevertheless, two options are available: (i) to perform dedicated high-resolution simulations (50 km or less) and detect tropical cyclones using object tracking algorithms, or (ii) to exploit existing low-resolution climate projections by looking for links between cyclone activity (in monthly mean) and the large-scale environment (cyclogenesis indices).

In Cattiaux et al. (2020), we explored these two approaches, with a focus on the Southern Indian Ocean. On the one hand, we performed dedicated experiments with the CNRM-CM6-1 atmospheric model in a rotated-stretched configuration (resolution up to 12 km over the area of interest), capable of producing realistic cyclones. In a 2 K-warmer world, the model simulates a 20% decrease in the frequency of tropical cyclones in the basin, associated with a slight poleward shift in their trajectories (Fig. 10a), together with an increase in their maximum intensity and a reduction of about one month in the period of cyclonic activity (later onset, Fig. 10c). On the other hand, we calculated the cyclogenesis indices in these dedicated simulations and in the CMIP5 multi-model projections (lower resolution). The indices do not capture the decrease in frequency, but partially represent the changes in geographical (Fig. 10b) and seasonal (Fig. 10c) distribution.

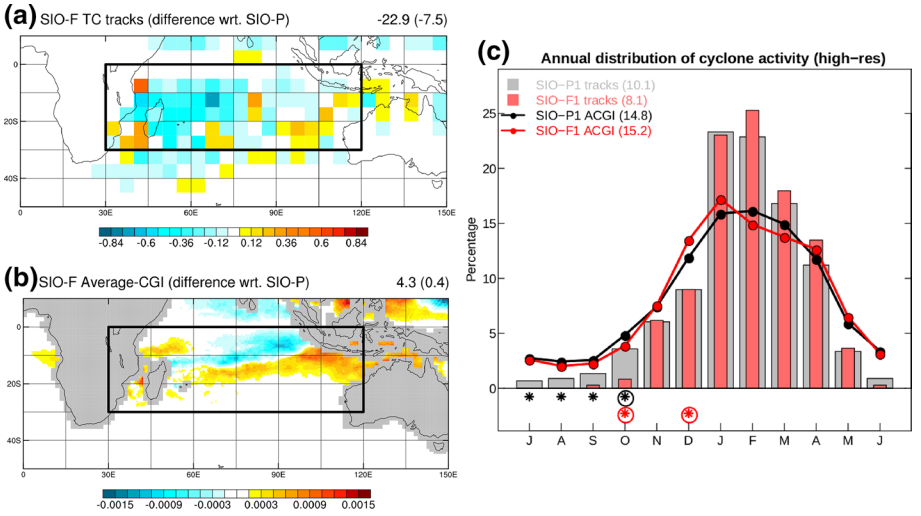

Fig. 10 Future evolution of TCs in the Indian Ocean. **a** Difference in track densities between future and present simulations. On average over the basin, we find a 20% decrease in the number of cyclone days (i.e. 7.5 days less). **b** Difference in cyclogenesis indices between present and future simulations. The indices miss the average decrease (they give + 0.4 days over the basin), but suggest the southward shift observed in a). **c** Annual distribution of cyclones (bars) and cyclogenesis indices (lines) for present (grey/black) and future (red) simulations. A significant decrease at the beginning of the season (October) and a significant increase at the end of the season (February to April) are visible

These results are consistent with a similar study on the North Atlantic (Chauvin et al. 2019), and, more generally, with the scientific literature (e.g. Camargo et al. 2014). The originality here lies in the focus on the South Indian Ocean (little studied so far) and the evidence of the reduction in the length of the cyclone season (important for monitoring and vigilance systems). Ongoing studies will give a better understanding the origins of the decrease in frequency projected by the model.

Further to the use of global climate models, another approach for evaluating future cyclonic risk is to estimate how damaging a recent historical cyclone could be if a similar one were to recur in the future (Schär 1996; Lackman 2015; Patricola 2018). In our case, we investigated Cyclone Bejisa, a climatologically typical cyclone that affected Reunion Island in early January 2014. Future environments for simulations of Bejisa-like cyclones were constructed using CMIP5 models to calculate changes in atmospheric and oceanic conditions, such as humidity and SST, between the recent climate and that of the end of the twenty-first century.

These changes were then added to ECMWF atmospheric and Mercator ocean analyses to create modified analyses of a future environment, thus permitting present versus future simulations. We conducted such simulations using the non-hydrostatic model Meso-NH with 3-km grid spacing, coupled to the ocean model CROCO for six different future environments derived from six different CMIP5 models.

Our findings suggest that future Bejisa-like cyclones will be 7% more intense, as measured by their maximum surface wind speed (Fig. 11a). Furthermore, the latitude at which future cyclones attain their lifetime maximum intensity will be displaced 2° further poleward, in line with an expansion of the tropics. In terms of trajectory, no substantial change was detected, as the present-day wind pattern was left unperturbed in order to maintain a north–south track that impacted Reunion Island. However, future cyclones were found to produce more intense rainfall, with the rainfall rates increasing by 29% on average (Fig. 11b). Additionally, future cyclones are predicted to be 9% smaller, as measured by the radius of their 17.5 m s^{-1} winds. However, further high-resolution studies are still needed to constrain this characteristic change, as large variability persists in the literature (Knutson

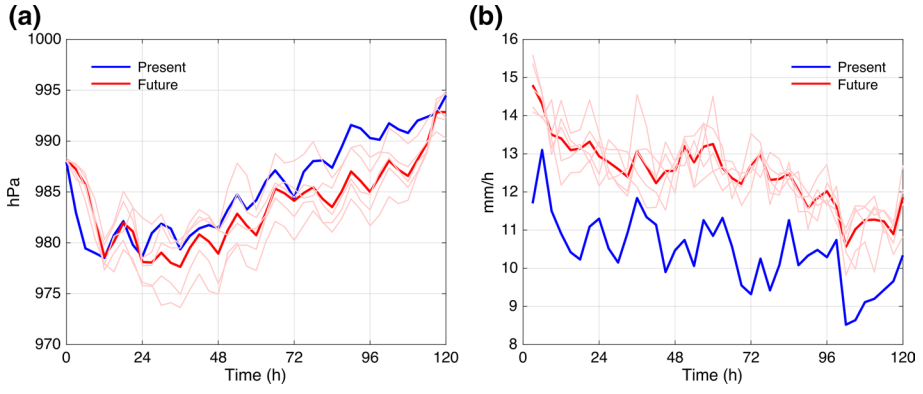

Fig. 11 Mean sea level pressure (**a**) and average rainfall rate within 100 km (**b**) of Bejisa-like cyclones simulated in Meso-NH coupled to the ocean model CROCO. A resimulation of Cyclone Bejisa in its historical environment (blue) is compared to Bejisa-like cyclones simulated in future environments derived from Coupled Model Intercomparison Project 5 (CMIP5) models (thin red lines) and their ensemble mean (red line). Projections indicate that such a typical cyclone could be characterized by significantly lower pressures and significantly heavier rainfalls in the future

2020). In addition to these atmospheric-related characteristics, we project a 0.2 m average increase in the significant ocean wave height, calculated by running the wave model WAVEWATCH III using hourly surface wind output. To the best of our knowledge, this is the first time that future changes in ocean waves have been projected for this basin. Although the change found here is modest, larger changes are anticipated for simulations based on stronger historical cyclones, with Cyclone Bejisa representing only a moderate-strength cyclone.

4 ReNovRisk database

The Sentinel remote sensing images produced during the RNR-I project have been processed and are stored on the servers and storage spaces of the SEAS-OI station, on which the project team relies (http://www.seas-oi.fr/en/web/guest/accueil). The SEAS-OI station is part of the French SEAS network of direct reception antennas for satellite data.

The SAR Sentinel-1 database is made up of data in the raw state or after different levels of pre-processing (spatial cropping and tiling, time filters) and processing (NDR, binary images, temporal summaries, etc.). Sentinel-2 optical data consist of raw L1C images, reflectance L2A images, cloud masks, multiple indices, and the results of change detection algorithms (classifications, temporal summaries, etc.). For each tile, covering an area of 100 km by 100 km, the entire time series (2015–2020) represents approximately 2 TB and more than 10,000 images. These numbers must be multiplied according to the geographical area and the number of S2 tiles monitored in the frame of the ReNovRisk programme.

These data from change detection chains therefore occupy very large volumes, which should be well organized to ensure a good perennial management. Work is underway to secure their storage and archiving, which currently rely mainly on the SEAS-OI infrastructure with a capacity of a few hundred TB. In addition, the metadata for each processing level is being produced to allow the harvesting of this image database. Finally, reflection is in progress to facilitate the availability of this data and, in particular, the final products (indices, change detection products), through a mapping web platform.

OSU-R (Observatoire des Sciences de l'Univers de la Reunion, CNRS, Météo-France and Université de la Reunion) organizes and supports transdisciplinary environmental research and operates a service unit (operation and maintenance of the stock of instruments, data analysis and processing). One goal of the services is the management of long-term observational data performed by its stations (that are part of European research infrastructures) and of measurement campaign datasets like the one produced in the framework of ReNovRisk. This data management is organized around 4 themes: data storage, metadata management, data processing, and data accessibility. The data storage provides long-term support and a backup guarantee, with an access by FTP for scientists and URL for data in open access. Metadata management is performed by means of OSU-R software, which allows information describing instrumentation and processing to be stored. The data processing is done through a data flow management service based on the Apache Airflow software (https://airflow.apache.org/), which pushes data to processing servers and data processing libraries, and classifies the data thus created. Finally, accessibility is achieved through the "GeOsur" tool (https://geosur.univ-reunion.fr), a web interface that aims to ensure the visibility of all the data produced. It is based on the open source software GeoNetwork (https://geonetwork-opensource.org) and allows the user to navigate easily through the database, using a search engine to visualize the different information on

the datasets, as well as the download links. This tool is based on standard data exchange protocols (ISO19139, OGC https://www.ogc.org), which allows it to be harvested to other institutional portals.

The ReNovRisk programme participates in an open science approach by making the data produced on cyclone risk available to the public. All this data management allows us to reference all the project data within the same catalogue. It will group together the data stored locally, and also data found in other databases. Finally, thanks to its interoperability, GeOsur will facilitate the transversal use of this data, both in the research field and for a wider audience. A demonstration of this interoperability is the harvesting of ReNovRisk data by another portal: PEIGO (http://peigeo.re), which is managed by AGORAH (http://www.agorah.com), the urban planning agency of Reunion Island, which aims to restore observational data in the form of cross-analyses to inform public policies.

5 Conclusions and perspectives

ReNovRisk is the first transdisciplinary programme dedicated to the study of cyclonic hazards in the Western Indian Ocean. It is composed of 4 different sub-programmes.

The first component, RNR-C, has enabled the development of new observation networks in the basin and numerical models for tropical cyclone modelling on the SWIO. The deployment of a GNSS network is intended to improve the state of the atmosphere in numerical weather prediction models through data assimilation. An intensive observation campaign was deployed in 2019 in the SWIO. New observation tools, in particular installed on marine and aerial drones, were tested in the environment of tropical cyclone Joaninha. Important numerical developments focused on the ocean–wave–atmosphere interactions, and on the representation of clouds and precipitation. The first studies have demonstrated the robustness of the modelling system, and a significant improvement in the track and intensity of the modelled tropical cyclones. ReNovRisk has also enabled high-resolution regional climate simulations for the SWIO, which have provided first answers to questions concerning the occurrence and geographical distribution of tropical cyclones in the coming decades. Moreover, high-resolution simulations of tropical cyclone Bejisa in a future climate have shown that its maximum intensity would be attained 2° further poleward, its intensity would increase by ~ 7%, and the precipitation rate would be strongly increased (~ 30%).

While RNR-C is planned to end in June 2021, the three other ReNovRisk sub-programmes are still in progress. Although they have not yet presented their final results, several scientific advances can be highlighted.

RNR-T is a first attempt to describe the integrated chain of tropical cyclone risks along a transect extending across the western volcanic plateau of Reunion Island (2000 m asl) and sloping down through ravines to the coastline. Infrastructures and preserved natural sites along the western coastal line of Reunion Island are particularly prone to overlapping cyclonic hazards (wind gusts, high precipitation, floods by ravines, transport of sediment, sea swell and submersion). A novel approach will involve cross-expertise in different domains (atmospheric physics, hydrology, sedimentology, geomorphology, coral reef growth, and ocean sciences). Complementary datasets will be required for calibrating model tools. Rainfall based on radar data corrected with rain gauge data will be estimated for catchments for which only a small number of point flow measurements are available.

RNR-E is a programme that focuses on the consequences of cyclones with the study, from upstream to downstream, of the sedimentary stock linked to ground movements and to flood-induced solid transport. The dynamics studied are characterized by different complementary methodologies. Thus, high-precision topographic surveys (GNSS network, geodetic marker, photogrammetry, and LiDAR) and seismological and electromagnetic measurement campaigns are being carried out on several landslides and rivers. Hydrological and geochemical monitoring of groundwater and surface water has also been implemented, and a broadband seismic network is monitoring the continuous transport of erosion products in rivers through the associated seismic noise. These data have made it possible to quantify, in particular with numerical modelling, precipitation and groundwater contributions to the acceleration of landslides during cyclonic events (Belle et al. 2014, 2018).

The remote sensing part of the RNR-I project has focused on the development of change detection algorithms to highlight the direct impacts of cyclones from satellite data. In order to promote their use by the largest possible number of interested parties, the processing chains developed are based on freely accessible Sentinel satellite data and are themselves published and open source. The data used come from the ESA Sentinel 1 and 2 satellites, acquired at high spatial (10 m) and temporal (5–10 day) resolutions with global coverage. Sen1Chain is the first processing chain developed that is based on SAR Sentinel 1 satellite data. It allows rapid detection of flooded areas by computing the normalized difference ratio (NDR) between two images, pre- and post-event. Based on radar data, Sen1Chain has the advantage of being insensitive to clouds, often numerous in a cyclonic context. The second processing chain developed, Sen2Chain, uses Sentinel 2 optical data to detect changes in land cover with a change vector analysis (CVA) method. As with Sen1Chain, Sen2Chain makes it possible to highlight floods linked to rainfall, but also modifications in plant cover under the action of the wind, or the appearance of bare ground. The greater sensitivity of this method to clouds is partly compensated by the high temporal acquisition frequency (5 days) increasing the probability of obtaining better quality images. Since 2015, the availability and historical depth of the Sentinel image database have allowed both processing chains to operate large time series of hundreds of images to place events in a seasonal context and highlight their exceptional nature. Several recent cyclonic events have been analysed in Madagascar (Enawo-2017 / Ava-2018), as have other events and geographical areas (Idai in Mozambique-2019, Dorian in the Bahamas—2019), on which the processing chains have demonstrated their effectiveness (Alexandre et al. 2020).

Beyond these thematic results, a significant contribution of ReNovRisk has been the networking of many scientists from different domains around collaborative programmes. ReNovRisk has brought together atmospheric physicists, hydrogeologists, geomorphologists, geophysicists, geomaticians, and economists to jointly analyse cyclonic hazards and impacts on Reunion Island and on the SWIO. These transdisciplinary collaborations have led to the development of a large set of tools to characterize the cyclonic hazards (wind, precipitation, swell) and their impacts after landfall (floods, landslides, coastline, sedimentary stock).

Furthermore, an important action of ReNovRisk is training and the communication of results. Two interoperable databases (GeOsur and Seas-OI) are under construction for free open access to the programme data with a horizon of mid-2021. Specific products developed for decision-makers and land-use planning institutes in Reunion Island will support adaptation to cyclonic hazards. Training activities are being carried out on the various scientific themes and on the tools deployed during ReNovRisk for students from SWIO countries (Mozambique and Madagascar).

ReNovRisk is intended to continue as the stakes are high for countries subject to cyclonic hazards, particularly in the SWIO, where the economic and health consequences of cyclones are significant in terms of poverty and infrastructure. As far as possible, ReNovRisk will be expanded more broadly into the fields of ecology, health, and social sciences, as the adaptation of territories to cyclone risks is a key element in building resilience to climate change.

Acknowledgements ReNovRisk was funded by the European Union through the ERDF and INTER-REG5 programmes, the région Reunion, the French state through the CPER programme, the University of Reunion, the BRGM, the IRD and the CNRS. Numerical modelling was made possible thanks to the computer resources of Météo-France. The authors would like to thank all the participants of the ReNovRisk programme.

Author contributions All the authors made significant contributions to the document through their participation in the ReNovRisk programme, the exploitation of data or numerical tools and the production of results. All authors contributed to the writing of the paper.

Funding ReNovRisk was funded by the European Union through the ERDF and INTER-REG5 programmes, the Reunion region and the French state through the CPER programme, the University of Reunion, the BRGM, the IRD and the CNRS.

Data availability Data will be available on GeoSUR (https://geosur.univ-reunion.fr/web/) and Seas-Oi (http://www.seas-oi.fr/web/guest/acces-aux-donnees) web platform from mid-2021. Beforehand, the data used can be requested from the authors.

Code availability Numerical models are in open source and available on web platforms: http://mesonh.aero.obs-mip.fr/, https://www.umr-cnrm.fr/surfex/, http://polar.ncep.noaa.gov/waves/wavewatch/, http://www.croco-ocean.orgref and https://portal.enes.org/oasis

Compliance with ethical standards

Conflict of interest No conflict of interests.

Ethics approval All the authors assure to have respected the scientific standard ethics in accordance with the recommendations of the publisher.

Financial interests All authors certify that they have no affiliations with or involvement in any organization or entity with any financial interest or non-financial interest in the subject matter or materials discussed in this manuscript.

References

Alexandre C, Johary R, Catry T, Mouquet P, Révillion C, Srakotondraompiana S, Pennober G (2020) A sentinel-1 based processing chain for detection of cyclonic flood impacts. Remote Sens 12(2):252

Andreas EL, Edson JB, Monahan EC, Rouault MP, Smith SD (1995) The spray contribution to net evaporation from the sea: A review of recent progress. Boundary-Layer Meteorol 72:3–52. https://doi.org/10.1007/BF00712389

Aunay B, Rey A, Le Moigne B, Somoza K, Cance A, Salomero J (2018) Impacts de la tempête tropicale BERGUITTA sur La Reunion - Synthèse des investigations dans le cadre de la procédure de reconnaissance d'état de catastrophe naturelle. Rapport BRGM/RP-67604-FR

Baray JL, Courcoux Y, Keckhut P, Portafaix T, Tulet P, Cammas JP, Hauchecorne A, Godin Beekmann S, De Mazière M, Hermans C, Desmet F, Sellegri K, Colomb A, Ramonet M, Sciare J, Vuillemin C, Hoareau C, Dionisi D, Duflot V, Vérèmes H, Porteneuve J, Gabarrot F, Gaudo T, Metzger JM, Payen G, Leclair de Bellevue J, Barthe C, Posny F, Ricaud P, Abchiche A, Delmas R (2013) Maïdo observatory: a new high-altitude station facility at Reunion Island (21° S, 55° E) for long-term atmospheric remote sensing and in situ measurements. Atmos Meas Tech 6:2865–2877. https://doi.org/10.5194/amt-6-2865-2013

Barbary D, Leroux MD, Bousquet O (2019) The orographic effect of Reunion Island on tropical cyclone track and intensity. Atmos Sci Lett 20:e882. https://doi.org/10.1002/asl.882

Barruol G, Reymond D, Fontaine FR, Hyvernaud O, Maurer V, Maamaatuaiahutapu K (2006) Characterizing swells in the southern Pacific from seismic and infrasonic noise analyses. Geophys J Int 164:516–542. https://doi.org/10.1111/J.1365-246X.2006.02871.x

Barruol G, Davy C, Fontaine FR, Schlindwein V, Sigloch K (2016) Monitoring austral and cyclonic swells in the "Iles Eparses" (Mozambique Channel) from microseismic noise. Acta Oecologica 72:120–128. https://doi.org/10.1016/j.actao.2015.10.015

Baum RL, Reid ME (1992) Geology, Hydrology and Mechanics of the Alani-Paty Landslide, Manoa Valley, Oahu, Hawaii. USGS 92–501, 87

Bernardie S, Desramaut N, Malet JP, Gourlay M, Grandjean G (2015) Prediction of changes in landslide rates induced by rainfall. Landslides 12:481–494. https://doi.org/10.1007/s10346-014-0495-8

Belle P, Aunay B, Bernardie S, Grandjean G, Ladouche MR, Join JL (2014) The application of an innovative inverse model for understanding and predicting landslide movements (Salazie cirque landslides, Reunion Island). Landslides 11:343–355.

Belle P, Aunay B, Lachassagne P, Ladouche B, Join JL (2018) Control of tropical landcover and soil properties on landslides' aquifer recharge. Piezomet and Dyn Water. https://doi.org/10.3390/w10101491

Bister M, Emanuel KA (2002) Low frequency variability of tropical cyclone potential intensity 1 Interannual to interdecadal variability. J Geophys Res 107:4801. https://doi.org/10.1029/2001JD000776

Bordi I, Fraedrich K, Sutera A, Zhu X (2014) Ground-based GPS measurements: time behavior from half-hour to years. Theor and Appl Climatol 115:615–625

Botzen WJW, Deschenes O, Sanders M (2019) The economic impacts of natural disasters: a review of models and empirical studies. Rev Environ Econ and Policy 13(2):167–188.

Bousquet O, Lees E, Durand J, Peltier A, Duret A, Mekies D, Boissier P, Donal T, Fleischer-Dogley F, Zakariasy L (2020a) Densification of the ground-based GNSS observation network in the South-West Indian Ocean: current status, perspectives and examples of applications in meteorology and geodesy. Front Earth Sci 8:566105. https://doi.org/10.3389/feart.2020.566105

Bousquet O, Barbary D, Bielli S, Kebir S, Raynaud L, Malardel S, Faure G (2020b) An evaluation of tropical cyclone forecast in the Southwest Indian Ocean basin with AROME-Indian Ocean convection-permitting numerical weather predicting system. Atmos Sci Lett 21:e950. https://doi.org/10.1002/asl2.950

Bousquet O, Dalleau M, Bocquet M, Gaspar P, Bielli S, Ciccione S, Remy E, Vidard A (2020c) Sea turtles for ocean research and monitoring: overview and initial results of the STORM project in the Southwest Indian Ocean. Front Marine Sci 7:859 (**in press**)

Bu YP, Fovell RG, Corbosiero KL (2014) Influence of Cloud-Radiative Forcing on Tropical Cyclone Structure. J Atmos Sci 71:1644–1662.

Cattiaux J, Chauvin F, Bousquet O, Malardel S, Tsai CL (2020) Projected changes in the Southern Indian Ocean cyclone activity assessed from high-resolution experiments and CMIP5 models. J Clim 33(12):4975–4991. https://doi.org/10.1175/JCLI-D-19-0591.1

Camargo SJ, Tippett MK, Sobel AH, Vecchi GA, Zhao M (2014) Testing the performance of tropical cyclone genesis indices in future climates using the HiRAM model. J Climate 27:9171–9196. https://doi.org/10.1175/JCLI-D-13-00505.1

Camargo SJ, Hsiang SM (2015) Tropical cyclones: From the influence of climate to their socioeconomic impacts. In: M. Chavez, M. Ghil, and J. Urrutia-Fucugauchi, editors, Extreme Events Observations, Modeling, and Economics. Wiley, New York, ISBN 978–1–119–15701–4.

Caine N (1980) The rainfall intensity-duration control of shallow landslides and debris flows. Geografiska Ann: Series A, Phys Geograph 62(1–2):23–27

Cappa F, Guglielmi Y, Soukatchoff VM, Mudry J, Bertrand C, Charmoille A (2004) Hydromechanical modelling of a large moving rock slope inferred from slope levelling coupled to spring long-term hydrochemical monitoring: example of the La Clapière landslide (Southern Alps, France). J Hydrol 291:67–90.

Chauvin F, Pilon R, Palany P, Bel Madani A (2019) Future changes in Atlantic hurricanes with the rotated-stretched ARPEGE-Climat at very high resolution. Climate Dyn 54:947–972.

Coe JA, Ellis WL, Godt JW, Savage WZ, Savage JE, Michael JA, Kibler JD, Powers PS, Lidke DJ, Debray S (2003) Seasonal movement of the Slumgullion landslide determined from Global Positioning System surveys and filled instrumentation, July 1998-March 2002. Eng Geol 68:67–101.

Colomb A, Kriat T, Leroux MD (2018) The rapid weakening of very severe tropical cyclone hellen (2014). Month Weather Rev 147:2717–2737.

Corominas J, Moya J, Ledesma A, Lloret A, Gili JA (2005) Prediction of ground displacements and velocities from groundwater level changes at the Vallcebre landslide (Eastern Pyrenees, Spain). Landslides 2:83–96.

Craig A, Valcke S, Coquart L (2017) Development and performance of a new version of the OASIS coupler, OASIS3-MCT_3.0. Geoscientific Model Development 10:3297–3308.

Davy C, Barruol G, Fontaine FR, Stutzmann E, Sigloch K (2014) Tracking major storms from microseismic and hydroacoustic observations on the seafloor. Geophys Res Lett. https://doi.org/10.1002/2014GL062319

Davy C, Stutzmann E, Barruol G, Fontaine FR, Schimmel M (2015) Sources of secondary microseisms in the Indian Ocean. Geophys J Int 202:1180–1189.

Davy C, Barruol G, Fontaine FR, Cordier E (2016) Analyses of extreme swell events on La Reunion Island from microseismic noise. Geophys J Int 207:1767–1782.

De Lavenne A, Andréassian V, Thirel G, Ramos MH, Perrin C (2019) A regularization approach to improve the sequential calibration of a semidistributed hydrological model. Water Resour Res 55:8821–8839.

De Maria M, Sampson CR, Knaff JA, Musgrave KD (2014) Is tropical cyclone intensity guidance improving? Bull Amer Meteor Soc 95:387–398.

Dell M, Jones BF, Olken BA (2014) What do we learn from the weather? The new climate-economy literature. J Econ Lit 52(3):740–798

Dodet G, Castelle B, Masselink G, Scott T, Davidson M, Floc'h F, Jackson D, Suanez S (2018) Beach recovery from extreme storm activity during the 2013/14 winter along the Atlantic coast of Europe. Earth Surf Process Landforms. https://doi.org/10.1002/esp.4500

Dow JM, Neilan RE, Rizos C (2009) The International GNSS Service in a changing landscape of Global Navigation Satellite Systems. J Geodesy 83:191–198

Emanuel KA (1986) An air–sea interaction theory for tropical cyclones. part I: steady-state maintenance. J Atmos Sci 43:585–604. https://doi.org/10.1175/1520-0469(1986)043,0585:AASITF.2.0.CO;2

Emanuel KA (1988) The maximum intensity of hurricanes. J Atmos Sci 45:1143–1155. https://doi.org/10.1175/1520-0469(1988)045,1143:TMIOH.2.0.CO;2

Eyring V, Bony S, Meehl GA, Senior CA, Stevens B, Stouffer RJ, Taylor KE (2016) Overview of the design and experimental organization of the Coupled Model Intercomparison Project Phase 6 (CMIP6). Geosci Model Dev 9:1937–1958

Fernández-Merodo JA, García-Davalillo JC, Herrera G, Mira P, Pastor M (2012) 2D viscoplastic finite element modelling of slow landslides: the Portalet case study (Spain). Landslides. https://doi.org/10.1007/s10346-012-0370-4

Fontaine FR, Barruol G, Gonzalez A (2015) Rivière des Pluies Project, La Reunion Island, 2015–2018; RESIF - Réseau Sismologique et géodésique Français. http://dx.doi.org/https://doi.org/10.15778/RESIF.ZF2015

Fovell RG, Bu YP, Corbosiero KL, Tung W, Cao Y, Kuo H, Hsu L, Su H (2016) Influence of cloud microphysics and radiation on tropical cyclone structure and motion. Meteorol Monograph 56:11.1-11.27. https://doi.org/10.1175/AMSMONOGRAPHS-D-15-0006.1

Geiger T, Frieler K, Bresch DN (2017) A global data set of tropical cyclone exposure (TCE-DAT). GFZ Data Services. https://doi.org/10.5880/pik.2017.005

Gonzalez A, Fontaine FR, Barruol G, Recking A, Burtin A, Join JL, Delcher E, Michon L (2020) Seismic signature of a river flooding in La Reunion Island during the tropical cyclone Dumazile (March 2018), submitted to Geophysical Journal International

Gonzalez A (2019) Suivi sismologique de l'impact des cyclones sur la charge de fond de la Rivière des Pluies et de la Rivière du Mât à La Reunion, Ph. D. thesis, Université de La Reunion, 171 p.

Gonzalez A, Fontaine FR, Burtin A, Barruol G, Recking A, Join JL, Delcher E (2017) Seismic monitoring of the bedload transport in La Reunion Island rivers during tropical cyclones. EGU2017–5937, In, 19:14462. http://adsabs.harvard.edu/abs/2017EGUGA.1914462

Hoarau T, Barthe C, Tulet P, Claeys M, Pinty JP, Bousquet O, Delanoë J, Vié B (2018a) Impact of the generation and activation of sea salt aerosols on the evolution of Tropical Cyclone Dumile. J Geophys Res Atmos 123:8813–8831. https://doi.org/10.1029/2017JD028125

Hoarau T, Pinty JP, Barthe C (2018b) A representation of the collisional ice break-up process in the two-moment microphysics scheme LIMA v1.0 of Meso-NH. Geosci Model Dev 11:4269–4289. https://doi.org/10.5194/gmd-11-4269-2018

IPCC (2013) Climate Change 2013. The physical science basis. Contribution of Working Group I to the Fifth Assessment Report of the Intergovernmental Panel on Climate Change. In T. Stocker et al. (Eds.), (p. pp. 1535). Cambridge University Press. doi: https://doi.org/10.1017/CBO9781107415324

Iverson RM, Major JJ (1987) Rainfall, ground-water flow, and seasonal movement at Minor Creek landslide, northwestern California: physical interpretation of empirical relations. Bull Geol Soc Am 99:579–594. https://doi.org/10.1130/0016-7606(1987)99%3c579:RGFASM%3e2.0.CO;2

Iverson RM (2000) Landslide triggering by rain infiltration. Water Resour Res 36(7):1897–1910

Hallegate S (2014) Natural Disasters and Climate Change, Springer International Publishing, XXII, 194 pp, doi:https://doi.org/10.1007/978-3-319-08933-1__2

Holland GJ (1980) An analytic model of the wind and pressure profiles in hurricanes. Month Wea Rev 108:1212–1218

Holland G (1993) WMO/TC-No. 560, Report No. TCP-31, World Meterological Organization. Accessed: 17–03–2020, https://wmo.asu.edu/content/world-greatest-twenty-four-hour-1-day-rainfall.

Kossin J, Emanuel K, Vecchi G (2014) The poleward migration of the location of tropical cyclone maximum intensity. Nature 509:349–352. https://doi.org/10.1038/nature13278

Kossin J, Knapp KR, Olander TL, Velden CS (2020) Global increase in major tropical cyclone exceedance probability over the past four decades. Proceedings of the National Academy of Sciences May 2020, 201920849; DOI: https://doi.org/10.1073/pnas.1920849117

Hsiang SM, Jina AS (2014) The Causal Effect of Environmental Catastrophe on Long-Run Economic Growth: Evidence from 6,700 Cyclones. Working Paper 20352, National Bureau of Economic Research. https://www.nber.org/papers/w20352

Hussain M, Chen D, Cheng A, Wei H, Stanley D (2013) Change detection from remotely sensed images: from pixel-based to object-based approaches. ISPRS J Photogramm and Remote Sens 80:91–106

Knutson T, Camargo SJ, Chan JCL, Emanuel K, Ho CH, Kossin J, Mohapatra M, Satoh M, Sugi M, Walsh K, Wu L (2020) Tropical cyclones and climate change assessment: part ii: projected response to anthropogenic warming. Bull Am Meteorol Soc. https://doi.org/10.1175/BAMS-D-18-0194.1

Lac C, Chaboureau JP, Masson V, Pinty JP, Tulet P, Escobar J, Leriche M, Barthe C, Aouizerats B, Augros C, Aumond P, Auguste F, Bechtold P, Berthet S, Bielli S, Bosseur F, Caumont O, Cohard JM, Colin J, Couvreux F, Cuxart J, Delautier G, Dauhut T, Ducrocq V, Filippi JB, Gazen D, Geoffroy O, Gheusi F, Honnert R, Lafore JP, Lebeaupin Brossier C, Libois Q, Lunet T, Mari C, Maric T, Mascart P, Mogé M, Molinié G, Nuissier O, Pantillon F, Peyrillé P, Pergaud J, Perraud E, Pianezze J, Redelsperger JL, Ricard D, Richard E, Riette S, Rodier Q, Schoetter R, Seyfried L, Stein J, Suhre K, Taufour M, Thouron O, Turner S, Verrelle A, Vié B, Visentin F, Vionnet V, Wautelet P (2018) Overview of the Meso-NH model version 5.4 and its applications. Geosci Model Dev 11:1929–1969. https://doi.org/10.5194/gmd-11-1929-2018

Lackmann GM (2015) (2015), Hurricane Sandy before 1900 and after 2100. Bull Amer Meteor Soc 96(4):547–560. https://doi.org/10.1175/BAMS-D-14-00123.1

Lafore JP, Stein J, Asencio N, Bougeault P, Ducrocq V, Duron J, Fischer C, Héreil P, Mascart P, Masson V, Pinty JP, Redelsperger JL, Richard E, Vilà-Guerau de Arellano J (1998) The Meso-NH atmospheric simulation system. part I: adiabatic formulation and control simulations. Ann Geophys 16:90–109. https://doi.org/10.1007/s00585-997-0090-6

Laurantin O (2008) Antilope: Hourly rainfall analysis merging radar and rain gauge data. Proc. Int. Symp. on Weather Radar and Hydrology Conf. 2008, Grenoble, France, Laboratoire d'étude des Transferts en Hydrologie et Environnement (LTHE), 2–8

Lecacheux S, Bonnardot F, Rousseau M, Paris F, Pedreros R, Lerma NA, Quetelard H, Barbary D (2018) Probabilistic forecast of coastal waves for flood warning applications at Reunion Island (Indian Ocean). J Coastal Res 85:776–780. https://doi.org/10.2112/SI85-156.1

Lees E, Bousquet O, Roy D, Leclair J (2020) Analysis of diurnal to seasonal variability of integrated water vapour in the South Indian Ocean Basin using ground-based GNSS and 5th generation ECMWF Reanalysis (ERA5) data. Q. J. R. Meteorol, Soc (**In press**)

Leroux M, Meister J, Mekies D, Dorla A, Caroff P (2018) A climatology of Southwest Indian ocean tropical systems: their number, tracks, impacts, sizes, empirical maximum potential intensity, and intensity changes. J Appl Meteor Climatol 57:1021–1041. https://doi.org/10.1175/JAMC-D-17-0094.1

Liébault F, Peteuil C, Remaître A (2010) Approches géomorphologiques de la production sédimentaire des torrents. Sciences Eaux & Territoires, n°2: 128–35. https://doi.org/https://doi.org/10.14758/SET-REVUE.2010.2.15

Lu J, Deser C, Reichler T (2009) Cause of the widening of the tropical belt since 1958. Geophys Res Lett 36(3):L03803

Mahabot MM, Pennober G, Suanez S, Troadec R, Delacourt C (2017a) Effect of tropical cyclones on short-term evolution of carbonate sandy beaches on Reunion Island. Indian Ocean J Coast Res 33(4):839–853

Mahabot MM, Jaud M, Pennober G, Le Dantec N, Troadec R, Suanez S, Delacourt C (2017b) The basics for a permanent observatory of shoreline evolution in tropical environments; lessons from back-reef beaches in La Reunion Island, Comptes Rendus Geoscience, 349(6–7). ISSN. https://doi.org/10.1016/j.crte.2017.09.010

Malet JP, Van Asch ThWG, Van Beek R, Maquaire O (2005) Forecasting the behaviour of complex landslides with a spatially distributed hydrological model. Nat Hazards and Earth Syst Sci 5:71–85. https://doi.org/10.5194/nhess-5-71-2005

Masson V, Le Moigne P, Martin E, Faroux S, Alias A, Alkama R, Belamari S, Barbu A, Boone A, Bouyssel F, Brousseau P, Brun E, Calvet JC, Carrer D, Decharme B, Delire C, Donier S, Essaouini K, Gibelin AL, Giordani H, Habets F, Jidane M, Kerdraon G, Kourzeneva E, Lafaysse M, Lafont S, Lebeaupin Brossier C, Lemonsu A, Mahfouf JF, Marguinaud P, Mokhtari M, Morin S, Pigeon G, Salgado R, Seity Y, Taillefer F, Tanguy G, Tulet P, Vincendon B, Vionnet V, Voldoire A (2013) The SURFEXv7.2 land and ocean surface platform for coupled or offline simulation of earth surface variables and fluxes. Geosci Model Dev 6:929–960. https://doi.org/10.5194/gmd-6-929-2013

Mavume AF, Rydberg L, Lutjeharms JRE (2008) Climatology of tropical cyclones in the South-West Indian Ocean; landfall in Mozambique and Madagascar. West Indian Ocean J Mar Sci 8:15–36

Meyer V, Becker N, Markantonis V, Schwarze R, Van den Bergh JCJM, Bouwer LM, Bubeck P, Ciavola P, Genovese E, Green C, Hallegatte S, Kreibich H, Lequeux Q, Logar I, Papyrakis E, Pfurtscheller C, Poussin J, Przyluski V, Thieken AH, Viavattene C (2013) Review article: assessing the costs of natural hazards - state of the art and knowledge gaps. Nat Hazards and Earth Syst Sci 13(5):1351–1373

Mile M, Benácek P, Rózsa S (2019) The use of GNSS zenith total delays in operational arome/hungary 3d-var over a central European domain. Atmosp Measure Techniq 12(3):1569–1579

Mittal R, Tewari M, Radhakrishnan C, Ray P, Singh T, Nickerson AK (2019) Response of tropical cyclone Phailin (2013) in the Bay of Bengal to climate perturbations. Clim Dyn 53:2013–2030. https://doi.org/10.1007/s00382-019-04761-w

Mouquet P, Alexandre C, Rasolomamonjy J, Rosa J, Catry T, Révillion C, Rakotondraompiana S, Pennober G (2020) SENTINEL-1 AND SENTINEL-2 time series processing chains for cyclone impact monitoring in South WestIndian Ocean. Int Arch Photogramm Remote Sens Spatial Inf Sci. https://doi.org/10.5194/isprs-archives-XLIII-B3-2020-1593-2020

Narayan PK (2003) Macroeconomic impact of natural disasters on a small island economy: evidence from a CGE model. Appl Econ Lett 10(11):721–723. https://doi.org/10.1080/1350485032000133372

Neumann CJ (1993) Global guide to tropical cyclone forecasting. Chap 1: Global overview. TD 560 - TCP 31, WMO, Genève, Suisse, 1.1–1.37

Ovadnevaite J, Manders A, de Leeuw G, Ceburnis D, Monahan C, Partanen AI, Korhonen H, O'Dowd CD (2014) A sea spray aerosol flux parameterization encapsulating wave state. Atmos Chem Phys 14(4):1837–1852. https://doi.org/10.5194/acp-14-1837-2014

Parent du Châtelet J, Tabary P, Guimera M (2005) The PANTHERE Project and the Evolution of the French Operational Radar Network and Products : Rain-estimation, Doppler winds, and Dual-Polarisation (Le projet PANTHERE), 32nd American Meteorological Society Radar Conference, Albuquerque, NM, http://ams.confex.com/ams/pdfpapers/96217.pdf

Parker CL, Bruyère CL, Mooney PA, Lynch AH (2018) The response of land-falling tropical cyclone characteristics to projected climate change in northeast Australia. Clim Dyn 51:3467–3485. https://doi.org/10.1007/s00382-018-4091-9

Patricola CM, Wehner MF (2018) Anthropogenic influences on major tropical cyclone events. Nature 563:339–346. https://doi.org/10.1038/s41586-018-0673-2

Pauthier B, Bois B, Castel T, Thévenin D, Smith CC, Richard Y (2016) Mesoscale and local scale evaluations of quantitative precipitation estimates by weather radar products during a heavy rainfall event, Advances in Meteorology, vol. 2016, Article ID 6089319, 9 pages

Pianezze J, Barthe C, Bielli S, Tulet P, Jullien S, Cambon G, Bousquet O, Claeys M, Cordier E (2018) A new coupled ocean-waves-atmosphere model designed for tropical storm studies: example of tropical cyclone Bejisa (2013–2014) in the south-west Indian ocean. J Adv Model Earth Syst. https://doi.org/10.1002/2017MS001177

Quetelard H, Bessemoulin P, Peterson TC, Burton A, Boodhoo Y, Cerveny RS (2007) WMO CCl Rapporteur for climate extremes decision, World Meteorological Organization. Accessed: 17–03–2020, https://wmo.asu.edu/content/

Raucoules D, de Michele M, Aunay B (2018) Landslide displacement mapping based on ALOS-2/PALSAR-2 data using image correlation techniques and SAR interferometry: application to the Hell-Bourg landslide (Salazie Circle, La Reunion Island). Geocarto Int. https://doi.org/10.1080/10106049.2018.1508311

Rault C, Dewez TJB, Aunay B (2020) Structure-from-motion processing of aerial archive photographs: sensitivity analyses pave the way for quantifying geomorphological changes since 1978 in La Reunion Island. ISPRS Ann. Photogramm Remote Sens Spatial Inf Sci 2:773–780. https://doi.org/10.5194/isprs-annals-V-2-2020-773-2020

Rotunno R, Emanuel KA (1987) An air-sea interaction theory for tropical cyclones. part II: evolutionary study using a nonhydrostatic axisymmetric numerical model. J Atmos Sci 44:542–561. https://doi.org/10.1175/1520-0469(1987)044%3c0542:AAITFT%3e2.0.CO;2

Rindraharisaona EJ, Cordier E, Barruol G, Fontaine FR, Singh M (2020) Assessing swells in La Reunion Island from terrestrial seismic observations, oceanographic records and offshore wave models. Geophys J Int 221:1883–1895. https://doi.org/10.1093/gji/ggaa117

Rojas-Serna C, Lebecherel L, Perrin C, Andreassian V, Oudin L (2016) How should a rainfall-runoff model be parameterized in an almost ungauged catchment? a methodology tested on 609 catchments, Water Resour. Res 52:4765–4784. https://doi.org/10.1002/2015WR018549

Schär C, Frei C, Lüthi D, Davies HC (1996) Surrogate climate-change scenarios for regional climate models. Geophys Res Lett. https://doi.org/10.1029/96GL00265

Schulz WH, McKenna JP, Kibler JD, Biavati G (2009) Relations between hydrology and velocity of a continuously moving landslide -evidence of pore-pressure feedback regulating landslide motion? Landslides 6:181–190. https://doi.org/10.1007/s10346-009-0157-4

SeityY BP, Malardel S, Hello G, Bénard P, Bouttier F, Lac C, Masson V (2011) The AROME-France convective-scale operational model. Mon Wea Rev 139:976–991. https://doi.org/10.1175/2010MWR3425.1

Staten PW, Lu J, Grise KM, Davis SM (2018) Birner T (2018) Re-examining tropical expansion. Nat Clim Change 8:768–775. https://doi.org/10.1038/s41558-018-0246-2

Staten PW, Grise KM, Davis SM, Karnauskas KB, Waugh DW, Maycock A, Fu Q, Cook K, Adam O, Simpson IR, Allen RJ, Rosenlof K, Chen G, Ummenhofer CC, Quan X, Kossin JP, Davis NA, Son S (2020) Tropical widening: From global variations to regional impacts. Bull Amer Meteor Soc 101(6):E897–E904. https://doi.org/10.1175/BAMS-D-19-0047.1

Strobl E (2012) The economic growth impact of natural disasters in developing countries: evidence from hurricane strikes in the Central American and Caribbean regions. J Dev Econ 97(1):130–141

Stumpf A, Augereau E, Delacourt C, Bonnier J (2016) Photogrammetric discharge monitoring of small tropical mountain rivers: a case study at Rivière Des Pluies, Reunion Island". Water Resour Res 52(6):4550–4570. https://doi.org/10.1002/2015WR018292

Tacher L, Bonnard C, Laloui L, Parriaux A (2005) Modelling the behaviour of a large landslide with respect to hydrogeological and geomechanical parameter heterogeneity. Landslides 2:3–14. https://doi.org/10.1007/s10346-004-0038-9

Tamura Y (2009) Wind-induced damage to buildings and disaster risk reduction. The Seventh Asia-Pacific Conference on Wind Engineering, November 8–12, 2009, Taipei, Taiwan

Terry J, Kim I-H, Jolivet S (2013) Sinuosity of tropical cyclone tracks in the South West Indian Ocean: spatio temporal patterns and relationships with fundamental storm attributes. Appl Geogr 45:29–40. https://doi.org/10.1016/j.apgeog.2013.08.006

Thompson C, Barthe C, Bielli S, Tulet P, Pianezze J Projecting Characteristic Changes of a Typical Tropical Cyclone under Climate Change in the South West Indian Ocean. Submitted to J. Geophys. Res.

Trabing BC, Bell MM, Brown BR (2019) Impacts of radiation and upper-tropospheric temperatures on tropical cyclone structure and intensity. J Atmos Sci 76:135–153. https://doi.org/10.1175/JAS-D-18-0165.1

Tulet P, Crassier V, Cousin F, Suhre K, Rosset R (2005) ORILAM, a three-moment lognormal aerosol scheme for mesoscale atmospheric model: online coupling into the Meso-NH-C model and validation on the Escompte campaign. J Geophys Res 110:D18201. https://doi.org/10.1029/2004JD005716

Vallet A, Charlier JB, Fabbri O, Bertrand C, Carry N, Mudry J (2016) Functioning and precipitation-displacement modelling of rainfall-induced deep-seated landslides subject to creep deformation. Landslides 13:653–670.

Van Asch TWJ, Buma J, Van Beek LPH (1999) A view on some hydrological triggering systems in landslides. Geomorphology 30:25–32.

Vérèmes H (2020) Application de la méthode dite « de bogus » dans le programme ReNovRisk-TRANSFERTS, Technical report, Université de La Reunion; Région Reunion. 2020. https://doi.org/10.26171/

Veron F (2015) Ocean sprays. Annu Rev Fluid Mech 47(1):507–538.

Vié B, Pinty JP, Berthet S, Leriche M (2016) LIMA (v10): a quasi two-moment microphysical scheme driven by a multimodal population of cloud condensation and ice freezing nuclei. Geosci Model Develop 9(2):567–586. https://doi.org/10.5194/gmd-9-567-2016

Vitart F, Ardilouze C, Bonet A, Brookshaw A, Chen M, Codorean C, Déqué M, Ferranti L, Fucile E, Fuentes M, Hendon H, Hodgson J, Kang HS, Kumar A, Lin H, Liu G, Liu X, Malguzzi P, Mallas I, Manoussakis M, Mastrangelo D, MacLachlan C, McLean P, Minami A, Mladek R, Nakazawa T, Najm S, Nie Y, Rixen M, Robertson AW, Ruti P, Sun C, Takaya Y, Tolstykh M, Venuti F, Waliser D, Woolnough S, Wu T, Won DJ, Xiao H, Zaripov R, Zhang L (2017) The seasonal to sub-seasonal forecast project database. Bull Am Meteor Soc 98:163–173. https://doi.org/10.1175/BAMS-D-16-0017.1

Voldoire A, Decharme B, Pianezze J, Lebeaupin Brossier C, Sevault F, Seyfried L, Garnier V, Bielli S, Valcke S, Alias A, Accensi M, Ardhuin F, Bouin MN, Ducrocq V, Faroux S, Giordani H, Léger F, Marsaleix P, Rainaud R, Redelsperger JL, Richard E, Riette S (2017) SURFEX v8.0 interface with OASIS3-MCT to couple atmosphere with hydrology, ocean, waves and sea-ice models, from coastal to global scales. Geosci Model Dev 10:4207–4227. https://doi.org/10.5194/gmd-10-4207-2017

WMO (2016) Tropical Cyclone Programme, Regional Association I –Tropical Cyclone Operational Plan for the South-West Indian Ocean. Report No. TCP-12, Report No. TCP-12, WMO-No. 1178, https://library.wmo.int/doc_num.php?explnum_id=4031

Authors and Affiliations

Pierre Tulet[1] · Bertrand Aunay[2] · Guilhem Barruol[3,4] · Christelle Barthe[1] · Remi Belon[2] · Soline Bielli[1] · François Bonnardot[5] · Olivier Bousquet[1] · Jean-Pierre Cammas[1,6] · Julien Cattiaux[7] · Fabrice Chauvin[7] · Idriss Fontaine[8] · Fabrice R. Fontaine[3,9] · Franck Gabarrot[6] · Sabine Garabedian[8] · Alicia Gonzalez[3,4] · Jean-Lambert Join[3] · Florian Jouvenot[10] · David Nortes-Martinez[8] · Dominique Mékiès[1] · Pascal Mouquet[10] · Guillaume Payen[6] · Gwenaelle Pennober[10] · Joris Pianezze[1] · Claire Rault[2] · Christophe Revillion[10] · Elisa J. Rindraharisaona[3,4] · Kevin Samyn[2] · Callum Thompson[1] · Hélène Vérèmes[1,6]

[1] LACy, Laboratoire de l'Atmosphère et des Cyclones (UMR 8105, Université de la Reunion, CNRS, Météo-France), Saint-Denis de La Reunion, France

[2] BRGM, Bureau de Recherches Géologiques et Minières, Saint-Denis de La Reunion, France

[3] LGSR, Laboratoire Géosciences Reunion (Université de La Reunion, IPGP), Saint-Denis de La Reunion, France

[4] Université de Paris, Institut de physique du globe de Paris, CNRS, Paris, France

[5] DIROI, Direction Interrégionale Océan Indien (Météo-France), Saint-Denis de la Reunion, France

[6] OSUR, Observatoire des Sciences de l'Univers de La Reunion (UMS 3365, Université de la Reunion, CNRS, Météo-France), Saint-Denis de la Reunion, France

[7] CNRM, Centre National de la Recherche Météorologique (UMR 3589, Météo-France, CNRS), Toulouse, France

[8] CEMOI, Centre d'Economie et de Management de l'Océan Indien (Université de la Reunion), Saint-Denis de La Reunion, France

[9] Université de Paris, Institut de physique du globe de Paris, CNRS F-75005 Paris, France. Observatoire volcanologique et sismologique de la Martinique, Institut de physique du globe de Paris, F-97250 Fonds Saint Denis, France

[10] Espace-Dev, Espace pour le Développement (UMR 228, IRD, Université de la Guyane, Université de La Reunion, Université des Antilles, Université de Montpellier), Montpellier, France